Journal of the American Heart Association

ORIGINAL RESEARCH

Pyruvate Kinase M2 Protects Heart from Pressure Overload-Induced Heart Failure by Phosphorylating RAC1

Le Ni, MD*; Bowen Lin, MD*; Lingjie Hu, MD; Ruoyu Zhang, Bsc; Fengmei Fu, Bsc; Meiting Shen, MD; Jian Yang, PhD; Dan Shi, MD, PhD

BACKGROUND: Heart failure, caused by sustained pressure overload, remains a major public health problem. PKM (pyruvate kinase M) acts as a rate-limiting enzyme of glycolysis. PKM2 (pyruvate kinase M2), an alternative splicing product of PKM, plays complex roles in various biological processes and diseases. However, the role of PKM2 in the development of heart failure remains unknown.

METHODS AND RESULTS: Cardiomyocyte-specific *Pkm2* knockout mice were generated by crossing the floxed *Pkm2* mice with α-MHC (myosin heavy chain)-Cre transgenic mice, and cardiac specific *Pkm2* overexpression mice were established by injecting adeno-associated virus serotype 9 system. The results showed that cardiomyocyte-specific *Pkm2* deletion resulted in significant deterioration of cardiac functions under pressure overload, whereas *Pkm2* overexpression mitigated transverse aortic constriction-induced cardiac hypertrophy and improved heart functions. Mechanistically, we demonstrated that PKM2 acted as a protein kinase rather than a pyruvate kinase, which inhibited the activation of RAC1 (rho family, small GTP binding protein)-MAPK (mitogen-activated protein kinase) signaling pathway by phosphorylating RAC1 in the progress of heart failure. In addition, blockade of RAC1 through NSC23766, a specific RAC1 inhibitor, attenuated pathological cardiac remodeling in *Pkm2* deficiency mice subjected to transverse aortic constriction.

CONCLUSIONS: This study revealed that PKM2 attenuated overload-induced pathological cardiac hypertrophy and heart failure, which provides an attractive target for the prevention and treatment of cardiomyopathies.

Key Words: heart failure ■ protein kinase ■ pyruvate kinase M2 ■ rho family, small GTP binding protein

Heart failure (HF) is a rapidly growing public health issue with an estimated prevalence of >30 million people globally.[1] Although guideline-recommended medical therapy has lowered the mortality of patients with HF,[2,3] the overall mortality and rehospitalization rates are still high.[3] Numerous studies have been undertaken to discover new mechanisms and develop therapeutic strategies aiming to improve the prognosis of HF. However, so far, few conceptual breakthroughs have been made.[4,5] Therefore, it's still urgent to reveal new and pivotal mechanisms contributing to HF.

Pyruvate kinase M (PKM) is the key enzyme responsible for converting phosphoenolpyruvate to pyruvate at the final step of glycolysis.[6] PKM1 and PKM2, 2 alternative-splicing isoforms of the *PKM* gene,[7,8] differ significantly in their protein structure and biochemical functions.[9,10] The tetramer of PKM2 exerts pyruvate kinase activity in glucose metabolism, whereas its monomer and dimer participate in multiple signaling pathways and cellular processes such as proliferation, migration, autophagy, and apoptosis independent of the pyruvate kinase activity.[11–14]

Correspondence to: Dan Shi and Jian Yang, Tongji University School of Medicine, 150 Jimo Road, Shanghai 200136, China.Email: shidan@tongji.edu.cn; jy279@tongji.edu.cn

*L. Ni and B. Lin contributed equally to this article.

Supplemental Material for this article is available at https://www.ahajournals.org/doi/suppl/10.1161/JAHA.121.024854

For Sources of Funding and Disclosures, see page 13.

JAHA is available at: www.ahajournals.org/journal/jaha

CLINICAL PERSPECTIVE

What Is New?

- PKM2 (pyruvate kinase M2) deficiency in cardiomyocytes accelerates the development of pressure overload-induced heart failure.
- PKM2 overexpression alleviates pressure overload-induced heart failure by modulating RAC1 (rho family, small GTP binding protein)-MAPK (mitogen-activated protein kinase) signaling pathway.
- PKM2 phosphorylates RAC1 in cardiomyocytes as a protein kinase, contributing to its cardioprotective effects.

What Are the Clinical Implications?

- This study unveils PKM2 as a cardioprotective protein kinase in maintaining cardiac homeostasis under hemodynamic stress overload, which offers a potential therapeutic target for heart failure.

Nonstandard Abbreviations and Acronyms

β-MHC	β-myosin heavy chain
cKO	conditional knockout
cTnT	cardiac troponin T
MAPK	mitogen-activated protein kinase
NRCM	neonatal rat cardiomyocytes
PKM1	pyruvate kinase M1
PKM2	pyruvate kinase M2
RAC1	rho family, small GTP binding protein

Several studies have documented that PKM2 exerts apparent cardioprotective potential in myocardial infarction and anthracycline-induced cardiotoxicity.[15,16] However, whether PKM2 plays any role in the progress of pressure overload HF is still unknown. In the present study, PKM2 deficiency exacerbated cardiac dysfunction of mice submitted to transverse aortic constriction (TAC), which was ameliorated by cardiomyocyte-specific PKM2 overexpression. Further investigation revealed that PKM2 inhibited the activation of RAC1 (rho family, small GTP binding protein) signaling pathway in cardiomyocytes by phosphorylating RAC1, contributing to its cardioprotective effects. Altogether, our findings highlight that PKM2 plays a novel role in protecting the heart from pressure overload-induced HF and PKM2-mediated RAC1 phosphorylation might serve as a potential target for the treatment of HF.

METHODS

The raw data that support the findings of this study are available from the corresponding authors on request. The authors declare that all supporting data are available in the article and its online supplementary files.

TAC Mouse Model

All animal procedures were approved by the Ethics Committee of Tongji University School of Medicine. The surgery procedure was similar to previous studies with minor modifications.[17] Male C57/BL mice around 8 to 9 weeks old (21–25 g) were anesthetized with isoflurane (RWD, R510-22-4), endotracheal intubated and ventilated with 1.5 mL tidal volume, and 120 to 130 breaths per minute. A heating pad was applied to maintain the body temperature of mice at 37°C until they were fully awake. In this study, we applied retrosternal approach to minimize surgical injury. After exposing the aortic arch, a 27-gauge needle was tied against the aorta arch with a 6-0 silk suture and removed immediately to establish the constriction. Sham-operated procedure underwent a similar procedure without transverse aorta ligation.

Generation of Cardiomyocyte-Specific *Pkm2* Knockout Mice

To generate cardiomyocyte specific *Pkm2* conditional knockout (*Pkm2*-cKO) mice, the mice with *Pkm2* gene exon 10 flanked by 2 loxP sites (*Pkm2*$^{f/f}$) were purchased from the Jackson Laboratory (024048) and crossed with α-MHC (myosin heavy chain)-Cre transgenic mice expressing noninducible CRE in cardiomyocytes. Genotypes of offspring were confirmed by polymerase chain reaction with *Pkm2*$^{f/f}$ and *Cre* specific primers. The primer sequences for genotyping were listed in Table S1.

Pkm2 Overexpression Experiments

For cardiomyocyte specific gene delivery, the adeno-associated virus type 9 (AAV9)-cardiac troponin T (cTnT) system was selected. Recombinant AAV9-cTnT carrying mouse full-length *Pkm2* (AAV9-cTnT-m*Pkm2*) and scrambled AAV9-cTNT-null were constructed by Hanbio Biotechnology Co. Ltd. (Shanghai, China). One week after TAC surgery, 100 μL/mouse (1×10^{11} viral particles) viruses were injected via the tail vein under anesthesia as previously described.[18]

Echocardiography

Transthoracic 2-dimensional M-mode echocardiography was performed with the Vevo 770 High-Resolution In Vivo Micro-Imaging System. Mice were anesthetized by isoflurane inhalation through a mask with heart rate

over 350 beats per minute. Left ventricular wall thickness and chamber diameter were measured in systole and diastole periods from a long-axis view. Left ventricular (LV) internal end-diastolic diameter, LV internal end-systolic diameter, fractional shortening, ejection fraction, and other parameters were calculated. Echocardiography was monitored once a week for a consecutive 6 to 8 weeks.

Cardiomyocyte Isolation, Culture, and Treatment

Neonatal rat cardiomyocytes (NRCMs) and neonatal mouse cardiomyocytes were dissociated by enzyme digestion, purified by differential adherence, and cultured in high glucose DMEM (Gibco, C11995500BT) supplemented with 10% fetal bovine serum (Excell, FND500) and 1% penicillin-streptomycin (Gibco, 15070063) as previously described.[19] After 24 hours, the medium was replaced with fresh high glucose DMEM with 1% fetal bovine serum and 1% penicillin-streptomycin for cell maintenance.

Adult mouse cardiomyocytes (AMCMs) were isolated and seeded in glass-bottom culture plates precoated with laminin (Sigma, L2020) in accordance with a simplified Langendorff-free protocol.[20] The plates were centrifuged at 200 *g* for 2 min, and incubated at 37 °C with 5% CO_2 for 2 h to facilitate cell adhesion. Then, the AMCMs were proceeded to subsequent experiments.

NRCMs and AMCMs were transfected with small interference RNA (siRNA) against rat *Pkm2* or *Rac1* and mouse *Pkm1* (40 nmol/L) respectively with lipofectamine™ RNAimax transfection reagent (Invitrogen, 13778150). The siRNA sequences of *Rac1* and *Pkm1* were obtained from the previous publications.[21,22] The scrambled siRNA (40 nmol/L) was used as negative control. 48 hours after transfection, phenylephrine (100 μmol/L for NRCMs and 50 μmol/L for AMCMs; Sigma, PHR1017) was added to the culture medium for 24 h. Then cells were collected for subsequent analysis. The siRNA sequences were listed in Table S2.

RNA Extraction and Quantitative Real-Time Polymerase Chain Reaction Analysis

Total RNA was extracted from fresh hearts and NRCMs, using RNAiso plus reagent (Takara, 9109) according to the manufacturer's protocols, and quantified by a Nanodrop; 1000 ng of total RNA was used to generate cDNA with the PrimeScript RT reagent Kit (Takara, RR037A). For quantitative assessment of gene expression, Quantitative real-time polymerase chain reaction analysis was performed. Specific mRNAs were quantified by SYBR green real-time master mix (Toyobo, QPK-201) on ABI QuantStudio 6 real-time polymerase chain reaction system (Applied Biosystems) under standard manufacturer's protocol; $2^{-\Delta\Delta Ct}$ method was used and the data were expressed as arbitrary units normalized to internal reference gene expression. Published primer sequences[23,24] were used and listed in Table S3.

Western Blot

As previously described,[25] cells or tissues were homogenized in RIPA lysis buffer (Beyotime, P0013C) supplemented with protease and phosphatase inhibitors (Roche, 4906845001; Roche, 4693116001) on ice for 30 minutes. The total proteins were extracted and quantified by BCA protein assay kit (Beyotime, P0009). Proteins were denatured with lithium dodecyl sulfate sample buffer (Invitrogen, NP0007) and separated on 10% Bis-Tris gel (Invitrogen, NP0315BOX). The proteins were transferred to polyvinylidene difluoride membrane (Millipore, IPVH00010) and blocked with 5% nonfat milk at room temperature (RT) for 1 hour. Subsequently, the membranes were incubated with the primary antibodies at 4 °C overnight. The following day, the membranes were rinsed in TBS with 0.1% Tween20 (TBST) 3 times, per 5 minutes and then incubated with corresponding secondary antibodies conjugated with near-infrared dyes (Invitrogen, A32735; A21036) at RT for 1 hour. The images of blots were captured with an Odyssey imager (LI-COR, Biosciences). The protein bands were quantified by ImageJ software. Signal intensity was normalized to β-Actin expression. The primary antibodies were listed in Table S4.

Immunoprecipitation and liquid chromatography/mass spectrometry-mass spectrometry (LC/MS-MS)

Twenty-five milligrams of protein from neonatal mouse cardiomyocytes was incubated with an anti-PKM2 antibody or immunoglobulin G at 4℃ overnight, and then 50 μL protein A/G agarose (Beyotime, P2012) was added and rotated at 4℃ for 3 to 4 hours. The samples were centrifuged to remove the supernatant and washed with 1 mL PBS 5 times, followed by the addition of lithium dodecyl sulfate sample buffer (Invitrogen, NP0007) and antioxidant (Invitrogen, NP0005). The samples were then denatured and separated on 10% Bis-Tris gel (Invitrogen, NP0315BOX). After the gel was visualized by Coomassie brilliant blue staining to assess the success of the immunoprecipitation, the remaining samples were processed for LC/MS-MS. The data were processed by the comparative proteomics analysis software suite mascot daemon (v2.5.1).

Histology Analysis

Mice were heparinized and anesthetized before they were euthanized. Then hearts were dissected,

weighed and fixed in 4% (wt/vol) paraformaldehyde (Sigma, P1648) at 4 °C for 24 hour. Samples were embedded in paraffin and sectioned at 6-μm thickness. Hematoxylin and eosin staining was performed according to the manufacturer's protocol of the hematoxylin and eosin staining kit (Beyotime, C0105S). Alexa Fluor 594 conjugated-wheat germ agglutinin (Invitrogen, W11262) was added to the sections to measure cardiomyocyte cross-sectional area. For cross-sectional area calculation, about 200 to 250 cardiomyocytes from 4 to 5 randomly selected fields (magnification, ×400) were measured. For picrosirius red staining, heart sections were incubated with picrosirius red solution (Abcam, ab150681) at RT for 1 hour as described previously.[26] Four to five randomly selected fields (magnification, ×200) were examined for collagen volume fraction analysis.

Immunofluorescence

Cells were fixed in 4% paraformaldehyde for 20 minutes, permeabilized in PBS with 0.5% Triton X-100 (Sigma, T9284) for 15 minutes and then blocked with 5% goat serum (Gibco, 16210072) in PBS with 0.1% Tween 20 for 60 minutes. After being incubated with primary antibodies against PKM2 (1:100; Cell Signaling Technology, 4053) and RAC1 (1:200; Proteintech, 66122-1-Ig) at 4℃ overnight, cells were washed with PBS with 0.1% Tween 20 and incubated with Alexa Fluor conjugated secondary antibodies at RT for 1 hour in the dark. Next, cells were stained with DAPI (Sigma, D9542) for 5 minutes. Finally, images were captured by the Lecia SP8 laser confocal microscopy with DAPI, CY5, and FITC fluorescence excitation filters.

Pyruvate Kinase Assay

The pyruvate kinase activity was measured by a pyruvate kinase assay kit (Sigma, MAK072). Briefly, cells or tissues were homogenized with pyruvate kinase assay buffer and then spun (9600 *g*, 5 minutes) to clear cell debris. The supernatant was transferred to clear-bottom 96-well plate to examine pyruvate kinase activity by measuring absorbance at a wavelength of 570 nm. The results were calculated based on the standard curve generated with the same kit, and the kinase activity was normalized to the protein concentration of the lysate.

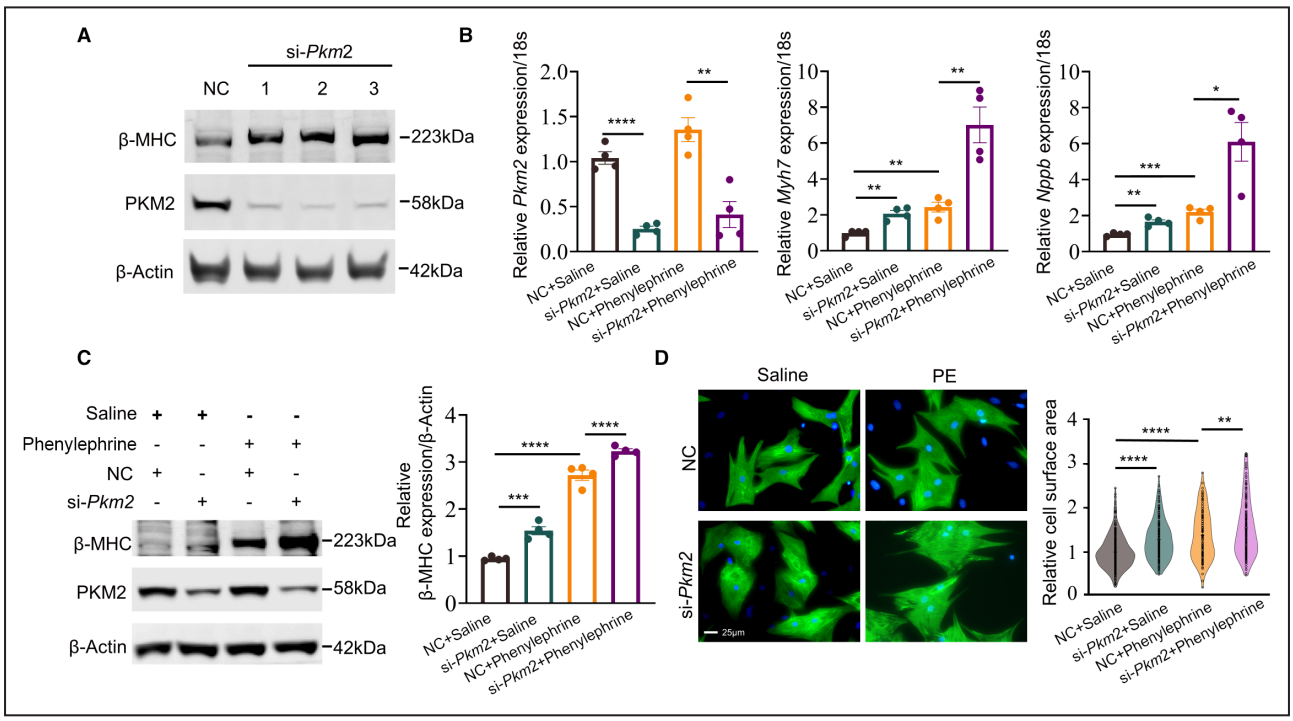

Figure 1. PKM2 (pyruvate kinase M2) deficiency exacerbates phenylephrine-induced cardiomyocyte hypertrophy in vitro. **A**, The interference efficiency of 3 *Pkm2* small interference RNAs (si-*Pkm2*) assessed by Western blot. β-actin served as loading control. **B**, Quantitative real-time polymerase chain reaction analysis of *Pkm2* and the cardiac hypertrophy markers *Myh7* (myosin heavy chain 7) and *Nppb* (natriuretic peptide precursor B) in neonatal rat cardiomyocytes coadministrated with phenylephrine and si-*Pkm2* sequence; *18S* was used as an internal reference gene, n=4. **C**, Western blot and quantification of cardiac β-MHC and PKM2 expression in neonatal rat cardiomyocytes coadministrated with phenylephrine and small interference RNA. β-actin served as loading control, n=4. **D**, Representative images and quantification of neonatal rat cardiomyocytes area (scale bar, 25 μm) from 4 groups (NC+Saline, n=285; si-*Pkm2*+Saline, n=172; NC+phenylephrine, n=131; si-*Pkm2*+phenylephrine, n=162). β-MHC indicates β-myosin heavy chain; NC, negative control; and PKM2-pyruvate kinase M2. Values represent as the mean±SEM; **P*<0.05, ***P*<0.01, ****P*<0.001, *****P*<0.0001.

Kinase Assay

The PKM2-mediated kinase reaction in vitro was performed as described previously.[27] Recombinant active-PKM2 (4 μg) (Abcam, ab89364) was incubated with 1 μg RAC1 (Abcam, ab89246) and phosphoenolpyruvate in 50 μL kinase buffer (Cell Signaling Technology, 9802) at 25 °C for 2 hours. The reactions were terminated by the addition of lithium dodecyl sulfate sample buffer. The reaction

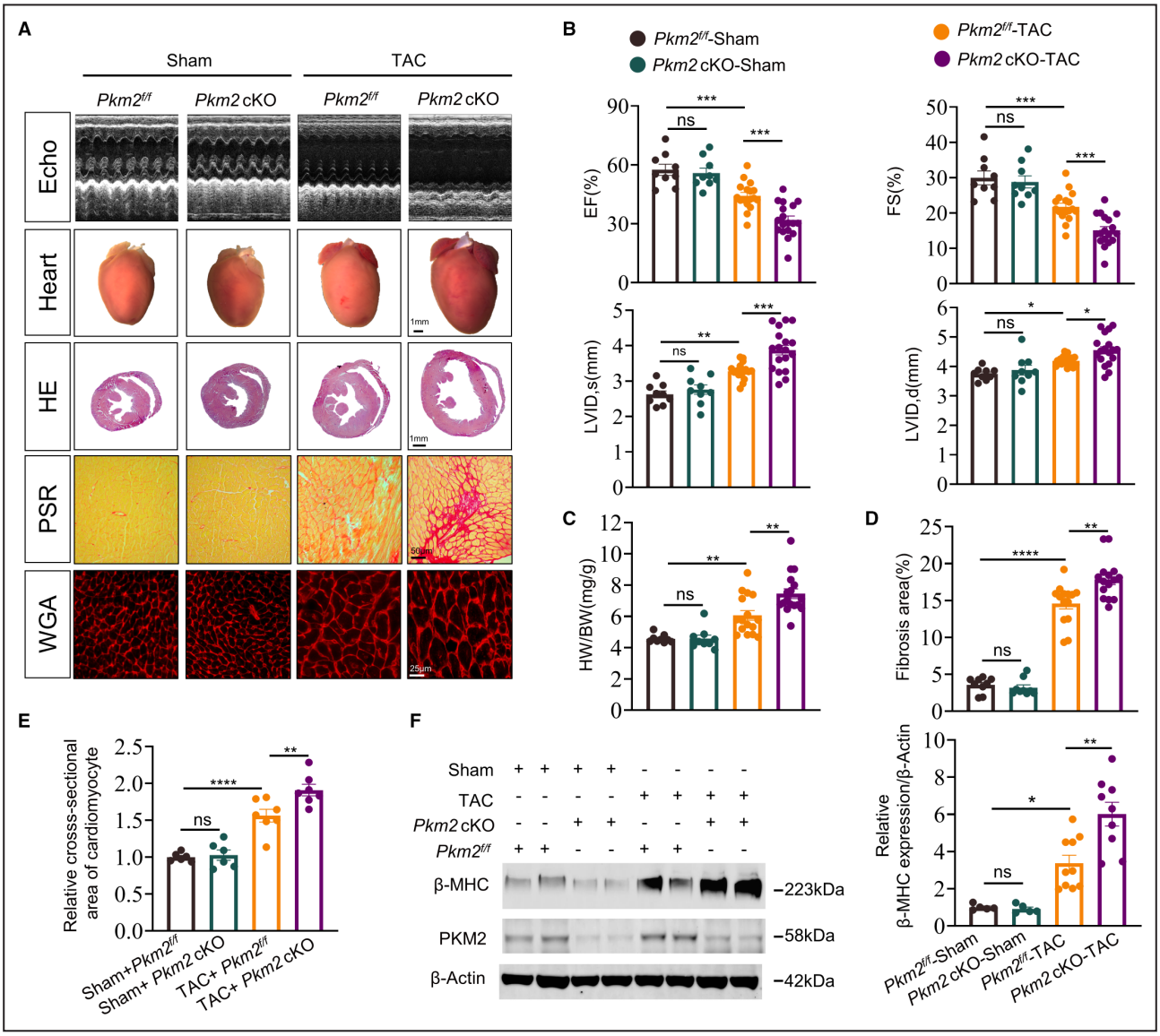

Figure 2. Cardiomyocyte-specific *Pkm2* (pyruvate kinase M2) knockout exacerbated pressure overload-induced heart failure in vivo.

A, Representative M-mode echocardiography, gross appearance of whole hearts (scale bar, 1 mm), heart cross-sections stained with hematoxylin and eosin (scale bar, 1 mm), histological analysis of heart sections by picrosirius red staining (scale bar, 50 μm), and cell boundaries demarcated with wheat germ agglutinin staining (scale bar, 25 μm) of *Pkm2* conditional knockout and *Pkm2*$^{f/f}$ mice 6 weeks after sham or transverse aortic constriction surgery. **B**, Quantitative analyses of echocardiography showing ejection fraction, fractional shortening, left ventricular internal end-systolic diameter, and left ventricular internal end-diastolic diameter , n=9 to 18. **C**, The ratio of heart weight to body weight, n=9 to 17. **D**, The sections were stained with wheat germ agglutinin to measure the cross-sectional area of cardiomyocytes, n=6 to 7. **E**, Statistical results of myocardial interstitial fibrosis analyzed by ImageJ software, n=9 to 15. **F**, Western blot and quantification of β-MHC expression of *Pkm2* conditional knockout and *Pkm2*$^{f/f}$ mice 6 weeks after sham or transverse aortic constriction surgery. β-actin served as loading control; n=5 to 9. β-MHC indicates β-myosin heavy chain; cKO, conditional knockout; EF, ejection fraction; FS, fractional shortening; HE, hematoxylin and eosin; HW/BW, heart weight to body weight; LVID, d, LV internal end-diastolic diameter; LVID, s, LV internal end-systolic diameter; *Pkm2*, pyruvate kinase M2; *Pkm2*$^{f/f}$, *Pkm2* gene flanked by 2 loxP sites; PSR, picrosirius red; RAC1, rho family, small GTP binding protein; TAC, transverse aortic constriction; and WGA, wheat germ agglutinin. Values represent as the mean±SEM; **P*<0.05, ***P*<0.01, ****P*<0.001, *****P*<0.0001.

mixtures were then analyzed by Phos-tag-PAGE (APExBIO, F4002), following the manufacturer's instructions.

Statistical Analysis

Data are represented as the mean±SEM from at least 3 different experiments. A *P* value <0.05 was considered statistically significant. Statistical analyses were conducted using unpaired or paired 2-tailed Student *t*-test, 1-way ANOVA, and 2-way ANOVA as appropriate by GraphPad Prism software 8.0 (GraphPad Software Inc).

RESULTS

Cardiomyocyte-Specific *Pkm2* Knockout Exacerbated Pressure Overload-Induced HF

To elucidate the importance of PKM2 in the process of cardiac hypertrophy and HF, we first performed *Pkm2* knockdown in NRCMs by RNA interference. All 3 siRNAs targeting *Pkm2* (si-*Pkm2*) exhibited significant interference efficiency and concomitantly increased the cardiac hypertrophic marker β-MHC (Figure 1A and Figure S1A). Among them, si-*Pkm2-2* was the most efficient one, we therefore selected si-*Pkm2*-2 for subsequent experiments. Remarkably, knockdown of *Pkm2* resulted in a potent cardiohypertrophic response, as reflected by elevated expression of cardiac hypertrophic markers (*Myh7* [myosin heavy chain 7] and *Nppb* [natriuretic peptide precursor B]), which was further exacerbated after phenylephrine treatment (Figure 1B). Concomitantly, expression of β-MHC protein showed a similar trend (Figure 1C). To confirm the cardiac hypertrophy phenotype, we examined the cell surface area of NRCMs. As shown in Figure 1D, *Pkm2*-deficient cardiomyocytes displayed larger cell surface area and were further enlarged upon phenylephrine stimulation.

Next, we generated *Pkm2* cardiomyocyte conditional knockout (cKO) mice by crossing $Pkm2^{f/f}$ mice with α-MHC-Cre mice for in vivo study. $Pkm2^{f/f}$ mice were used as control. Western blot and quantitative real-time polymerase chain reaction analysis verified that *Pkm2* was effectively knocked down in hearts of *Pkm2* cKO mice (Figure S1B and S1C). In addition, the cardiomyocyte-specific deletion of *Pkm2* was confirmed in AMCMs purified from *Pkm2* cKO mice (Figure S1D).

Li et al have reported that the expression of *Myh6* (myosin heavy chain 6) in cardiomyocytes was no earlier than E12.5 mouse embryo.[28] Considering the $Pkm2^{f/f}$::α-MHC-Cre cKO mice were generated via noninducible cKO strategy, whether loss of PKM2 affected embryonic development need to be elucidated. We therefore examined the hearts of *Pkm2* cKO mice at different developmental stages (E12.5, E16.5, E18.5, and P0). The gross appearance of the hearts, heart weight/body weight ratio, number of viable mice (Figure S2A through S2D) and expression cell proliferation markers (Ki67 and pH3) (Figure S2E through S2H) did not differ between $Pkm2^{f/f}$ and *Pkm2* cKO mice. Meanwhile, immunoblotting of heart tissues revealed that the expression of PKM2 was significantly reduced in E16.5, E18.5 embryos and neonates, but not in E12.5 embryos (Figure S2I through S2J). In view of this, *Pkm2* cKO mice did not manifest overt developmental and morphological defects in hearts at baseline.

We then randomly divided $Pkm2^{f/f}$ and *Pkm2* cKO mice into sham or TAC operation groups ($Pkm2^{f/f}$-sham, *Pkm2* cKO-sham, $Pkm2^{f/f}$-TAC, and *Pkm2* cKO-TAC). A significant difference in cardiac function was observed between $Pkm2^{f/f}$-TAC and *Pkm2* cKO-TAC groups 6 weeks after TAC (Figure 2A, 2B and Figure S3A through S3G). First, *Pkm2* cKO-TAC mice displayed more pronounced ventricular dilation than $Pkm2^{f/f}$-TAC mice, evidenced by increased LV internal end-diastolic diameter and LV internal end-systolic diameter dimension (Figure 2A and 2B). Meanwhile, ejection fraction and fractional shortening were significantly lower in *Pkm2* cKO-TAC mice, indicating that *Pkm2* deficiency worsens TAC-induced cardiac dysfunction (Figure 2A

Figure 3. PKM2 (pyruvate kinase M2) acted as a protein kinase to inhibit RAC1 (rho family, small GTP binding protein) activation.

(**A** through **C**) Western blot and quantitation of PKM2 and PKM1 (pyruvate kinase M1) expression in neonatal rat cardiomyocytes after *Pkm2* knockdown. β-actin served as loading control, n=4. **D**, Relative pyruvate production determined by an absorbance assay in NRCMs after *Pkm2* knockdown, n=4. **E**, Immunoprecipitation (IP) assay using anti-PKM2 antibody in neonatal mouse cardiomyocytes. **F**, Immunoprecipitation assay using anti-RAC1 antibody in neonatal mouse cardiomyocytes. **G**, Representative immunofluorescence images showing the colocalization of PKM2 (green) and RAC1 (red) in adult mouse cardiomyocytes and NRCMs by confocal immunofluorescence analysis (scale bars, 25 μm in adult mouse cardiomyocytes; 10 μm in NRCMs). Line profile analyses showing the distribution and intensity. The Pearson coefficient was measured from the images using ImageJ software (n=21). **H**, Representative Western blot and Coomassie brilliant blue staining showing the phosphorylation of RAC1 by PKM2 in vitro. Phosphoenolpyruvate was used as the phosphate donor. **I**, Western blot and quantitation of p-RAC1 (S71) expression in NRCMs after *Pkm2* knockdown. β-actin served as loading control. **J**, Western blot and quantitation of RAC1 protein expression in the cycloheximide chase experiment. β-actin served as loading control. AMCMs indicates adult mouse cardiomyocytes; IB, immunoblot; IgG, immunoglobulin G; IP, Immunoprecipitation; NC, negative control; NRCMs, neonatal rat cardiomyocytes; PKM1, pyruvate kinase M1; PKM2, pyruvate kinase M2; RAC1, rho family, small GTP binding protein; TAC, transverse aortic constriction; and WGA, wheat germ agglutinin. Values represent as the mean±SEM; **P*<0.05, ***P*<0.01,*****P*<0.0001.

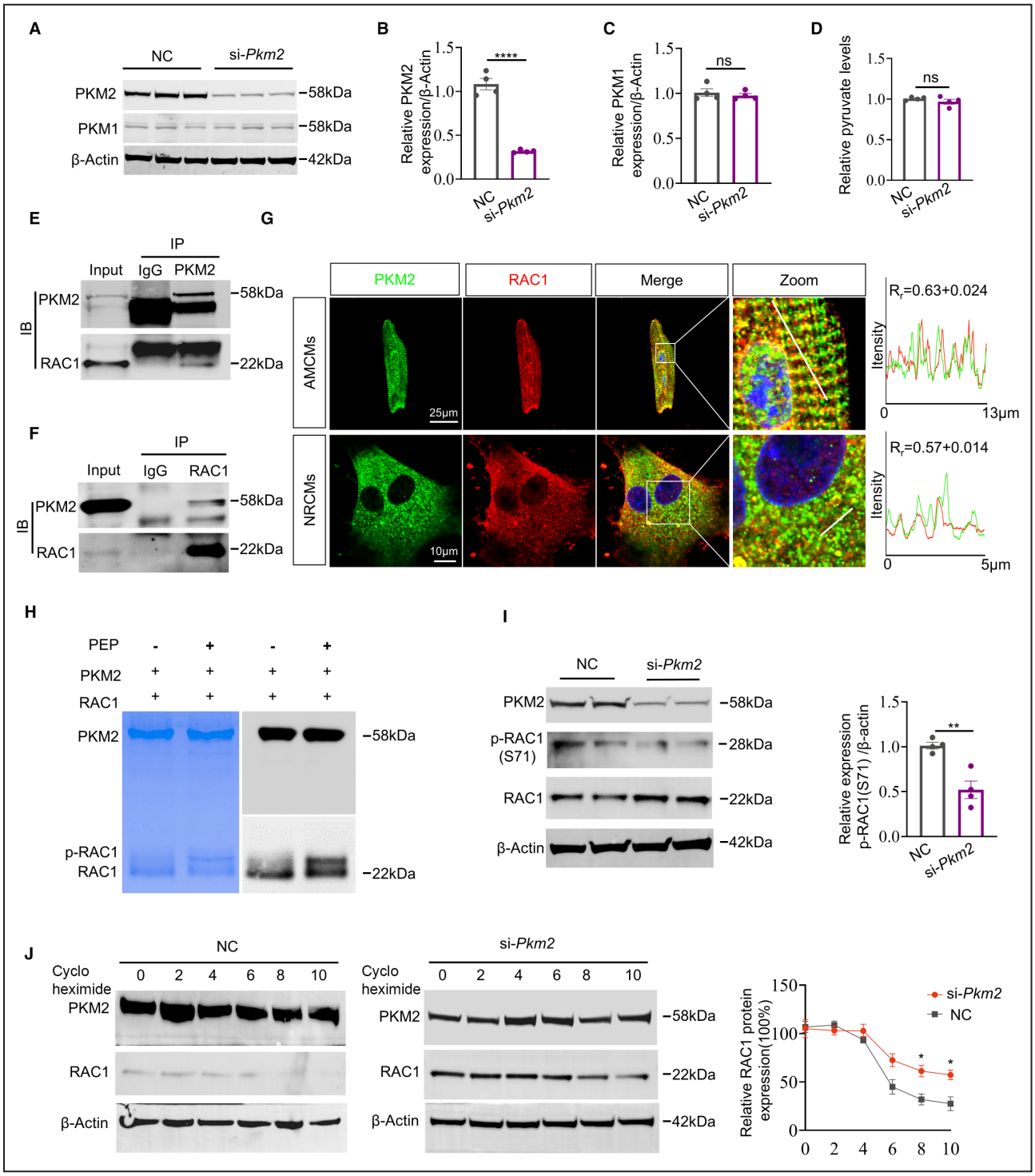

and 2B). After the echocardiography, the mice were euthanized, and the heart and body weight were measured, which showed that *Pkm2* cKO-TAC group had the highest heart weight/body weight ratio (Figure 2C). Stereomicroscope and hematoxylin and eosin staining further validated enlarged heart and dilated heart chambers in *Pkm2* cKO-TAC versus *Pkm2*$^{f/f}$-TAC mice (Figure 2A). Besides cardiac dysfunction and gross abnormal morphology, histologically, the progression of HF manifests cardiac hypertrophic growth and fibrosis. We then performed wheat germ agglutinin staining to measure the area of cardiomyocytes, and picrosirius red staining to assess the extent of fibrosis. Similarly, *Pkm2* cKO-TAC mice displayed more enlarged

cardiomyocytes and severer fibrosis (Figure 2D and 2E), accompanied by significantly elevated β-MHC in the hearts of *Pkm2* cKO-TAC mice compared with their controls (Figure 2F). These results suggested that PKM2-deficient hearts are susceptible to pressure overload-induced cardiac hypertrophy and HF.

PKM2 or PKM1 are translated from the same PKM mRNA by post-transcriptional splicing,[7,8] so we detected the expression of PKM, PKM1, and PKM2 in AMCMs purified from *Pkm2*$^{f/f}$ and *Pkm2* cKO mice with or without TAC operation. As indicated in Figure S4A, *Pkm2* cKO increased PKM1 and total PKM expression, which was consistent with previous reports by Magadum et al and Li et al.[15,29] Upon TAC operation, the expression of PKM2 and PKM1 was respectively increased and decreased accompanied by slight increase in PKM in *Pkm2*$^{f/f}$ mice, while in *Pkm2* cKO mice, increasing level of PKM and PKM1 was detected though still lower than those of *Pkm2* cKO sham mice (Figure S4A). Then, we investigated whether PKM1 contributes to the phenotype observed in PKM2 cKO hearts by using AMCMs purified from *Pkm2*$^{f/f}$ and *Pkm2* cKO mice. After successfully knockdown *Pkm1* expression in AMCMs with siRNA targeting *Pkm1*, PKM2-deficient AMCMs manifested severer cardiohypertrophic phenotype (as indicated by the expression of β-MHC) under phenylephrine stimulation (Figure S4B). Moreover, the overexpression of *Pkm1* was reported to improve the cardiac dysfunction induced by pressure overload.[29] The results above indicated that the upregulation of PKM1 in *Pkm2* cKO mouse heart is not sufficient to compensate for the phenotype caused by PKM2 deficiency under pressure overload, suggesting that PKM1 and PKM2 may also have nonredundant functions in pressure overload induced HF.

PKM2 Acted as a Protein Kinase to Inhibit RAC1 Activation

Considering the role of PKM2 in glycolysis, we first tested whether PKM2 deficiency impaired the glycolysis in cardiomyocytes. We measured the pyruvate

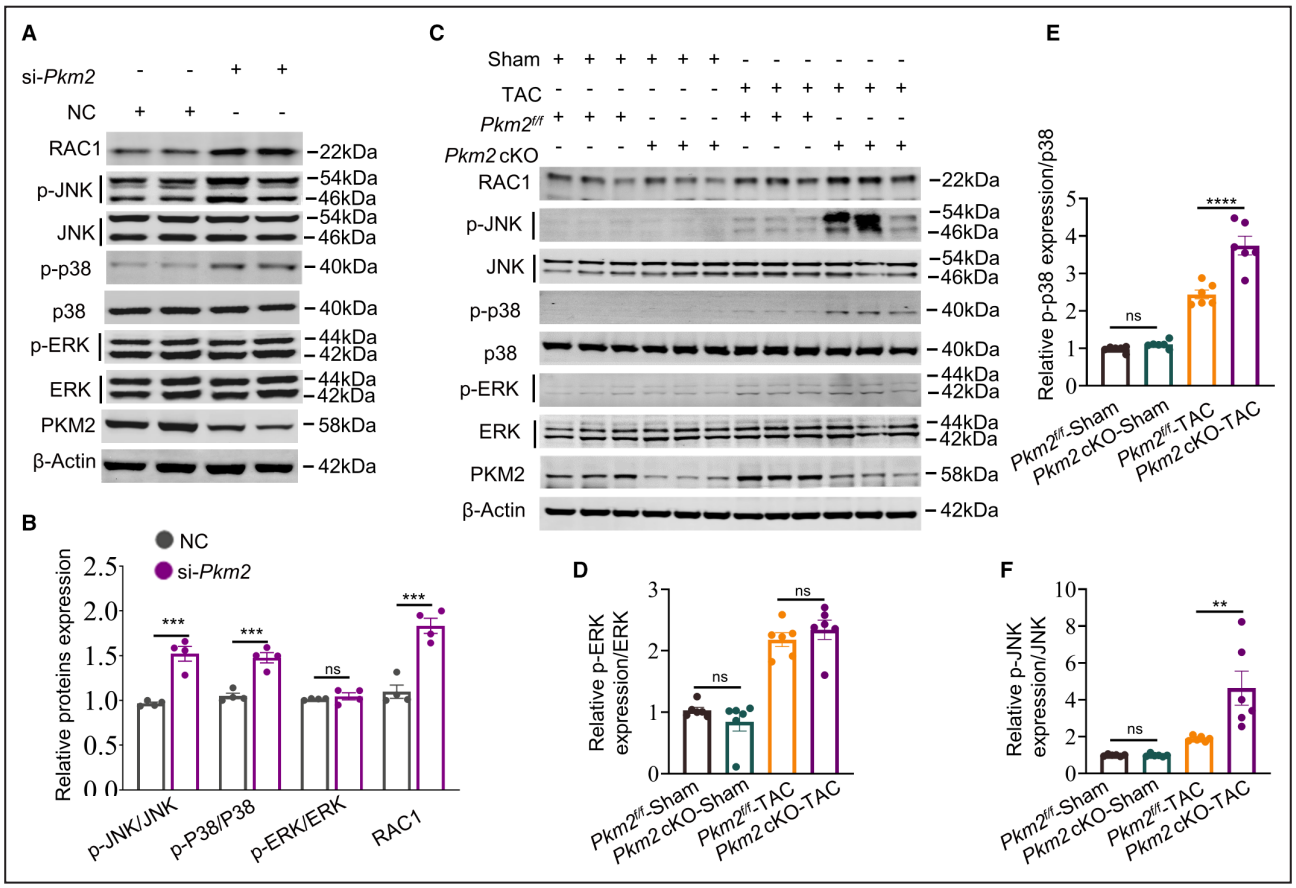

Figure 4. Cardiomyocyte-specific *Pkm2* (pyruvate kinase M2) deficiency activated RAC1 (rho family, small GTP binding protein)-MAPK signaling pathway in the progression of heart failure.
A and **B**, Western blot and quantification of phosphorylation of p38, p38, p-ERK, ERK, phosphorylation of JNK, and JNK in neonatal rat cardiomyocytes treated with si-*Pkm2* for 72 hours. β-actin served as loading control. **C** through **F**, Western blot and quantification of p-p38, p38, p-ERK, ERK, p-JNK, and JNK expression in heart tissues from *Pkm2* conditional knockout and *Pkm2*$^{f/f}$ mice 6 weeks after sham or transverse aortic constriction surgery. β-actin served as loading control. Minimum of n=6 per group. cKO indicates conditional knockout; *Pkm2*, pyruvate kinase M2; RAC1, rho family, small GTP binding protein; p-p38, phosphorylation of p38; and p-JNK, phosphorylation of JNK. Values represent as the mean±SEM; ***P*<0.01, ****P*<0.001, *****P*<0.0001.

kinase activity by detecting pyruvate production in cardiomyocytes. In *Pkm2* knockdown NRCMs, specific siRNA targeting *Pkm2* did not affect the expression of PKM1 (Figure 3A through 3C), which was consistent with previous work.[30] Meanwhile, pyruvate kinase activity remained unchanged between control and si-*Pkm2* groups (Figure 3D). These results indicated that PKM2 deficiency in cardiomyocytes did not impair pyruvate kinase activity. We then set to investigate the molecular mechanism of PKM2 in the

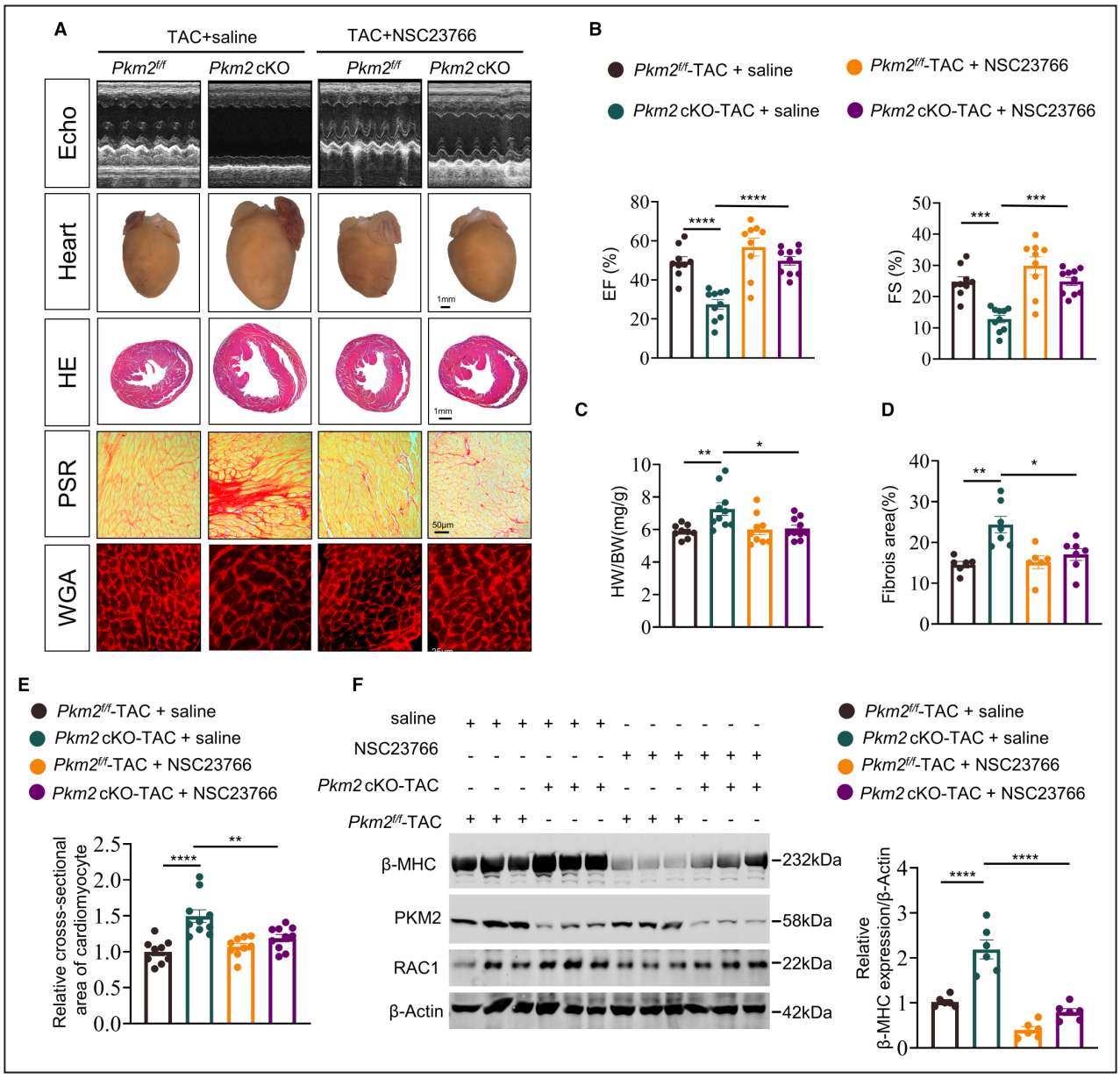

Figure 5. RAC1 (rho family, small GTP binding protein) inhibition mitigated pressure overload-induced heart failure.
A, Representative M-mode echocardiography, gross appearance of whole hearts (scale bar, 1 mm), heart cross-sections stained with hematoxylin and eosin (scale bar, 1 mm), histological analysis of heart sections by picrosirius red staining (scale bar, 50 μm) and cell boundaries demarcated with wheat germ agglutinin staining (scale bar, 25 μm) from *Pkm2* conditional knockout and *Pkm2*$^{f/f}$ mice after transverse aortic constriction surgery cotreated with saline or NSC23766. **B**, Quantitative analyses of echocardiography showing ejection fraction and fractional shortening, n=9 to 10. **C**, The ratio of heart weight to body weight, n=9 to 10. **D**, Statistical results for myocardial interstitial fibrosis analyzed by ImageJ software. n=6 to 7. **E**, Statistical results for the cell cross-sectional area, n=9 to 10. **F**, Western blot and quantification of β-MHC expression in hearts of *Pkm2* conditional knockout and *Pkm2*$^{f/f}$ mice after transverse aortic constriction surgery cotreated with saline or NSC23766. β-actin served as loading control. β-MHC indicates β-myosin heavy chain; cKO, conditional knockout; EF, ejection fraction; FS, fractional shortening; HE, hematoxylin and eosin; HW/BW, heart weight to body weight; *Pkm2*, pyruvate kinase M2; PSR, picrosirius red; RAC1, rho family, small GTP binding protein; TAC, transverse aortic constriction; and WGA, wheat germ agglutinin. Values represent as the mean±SEM; **P*<0.05, ***P*<0.01, ****P*<0.001, *****P*<0.0001.

progression of HF. By using an anti-PKM2 antibody-conjugated agarose assistant immunoprecipitation mass spectrometry, we identified about 230 proteins (sum phosphoenolpyruvate score > immunoglobulin G group) as putative partners of PKM2 in neonatal mouse cardiomyocytes (Table S5). By combining our immunoprecipitation mass spectrometry data with related studies,[31–34] we speculated that RAC1 might be one of the potential targets of PKM2 in regulating cardiac hypertrophy. We therefore selected RAC1 for further analysis. With PKM2 immunoprecipitation and Western blot, RAC1 was validated as the partner of PKM2 (Figure 3E). In a reciprocal immunoprecipitation experiment, endogenous PKM2 was also detected in immunoprecipitated RAC1 from neonatal mouse cardiomyocyte lysates (Figure 3F). We then examined the intracellular localization of PKM2 and RAC1 to further determine the relationship between PKM2 and RAC1 in situ. Consistent with immunoprecipitation results, endogenous PKM2 and RAC1 colocalized in the cytoplasm of NRCMs and AMCMs (Figure 3G).

Since the nonmetabolic function of PKM2, such as protein kinase, contributes to multiple tumor pathological processes,[11] we next examined the kinase activity of PKM2 on RAC1 phosphorylation. We performed in vitro kinase activity assay determined by a Phos-tag approach using purified active PKM2 and RAC1 proteins. Coomassie brilliant blue staining and immunoblot suggested that PKM2 was able to phosphorylate RAC1 (Figure 3H). Moreover, *Pkm2* knockdown caused a significant decrease in phosphorylated RAC1 at Serine 71 (p-RAC1 (S71)) in NRCMs (Figure 3I). p-RAC1 (S71) has been reported to lower the stability of RAC1 protein and accelerate its degradation,[35] which was confirmed by the cycloheximide chase assay showing that the half-life of the RAC1 protein in *Pkm2* knockdown NRCMs was significantly increased (Figure 3J).

Cardiomyocyte-Specific *Pkm2* Deficiency-Activated RAC1-MAPK Signaling Pathway in the Progression of HF

As a member of small guanine nucleotide-binding proteins of the Rho GTPase family (Rac, Cdc42, and Rho), RAC1 regulates the activity of MAPKs (mitogen-activated protein kinases), including p38, ERK, and JNK, which play important roles in pathological cardiac hypertrophy.[31–33] Therefore, we first investigated the expression and active phosphorylation of MAPKs in *Pkm2*-deficiency NRCMs. Immunoblot revealed that phosphorylation of p38 (p-p38) and JNK (p-JNK), but not p-ERK was increased in response to *Pkm2* knockdown-induced RAC1 elevation (Figure 4A and 4B). It has been reported that both p-p38 and p-JNK were significantly increased after TAC operation.[36,37] We then examined the expression and active phosphorylation of MAPKs in the hearts of $Pkm2^{f/f}$ and *Pkm2* cKO mice. While p-p38 and p-JNK displayed similar expression level in $Pkm2^{f/f}$ and *Pkm2* cKO mice at baseline, both proteins significantly increased in *Pkm2* cKO mice after TAC compared with controls (Figure 4C through 4F). Collectively, PKM2 deficiency in cardiomyocytes reduced RAC1 phosphorylation leading to enhanced RAC1 protein stability, which in turn activated the RAC1-MAPK signaling pathway.

Given the activated RAC1-MAPK axis in *Pkm2* cKO hearts, we postulated that RAC1 inhibition might delay pressure overloaded-induced HF in *Pkm2* cKO mice. To test this, we selected NSC23766, a specific inhibitor of RAC1. In NRCMs, NSC23766 significantly reduced *Pkm2* silencing induced β-MHC expression (Figure S5A). Similarly, *Rac1* knockdown also inhibited β-MHC expression in *Pkm2*-deficient NRCMs, whereas PKM2 expression was not affected (Figure S5B and Figure S5C). Increased expression of activated form of RAC1 has been reported in the pressure overloaded heart.[38] We then randomly treated $Pkm2^{f/f}$-TAC and *Pkm2* cKO-TAC mice with NSC23766 (2.5 mg/kg per

Figure 6. Cardiomyocyte-specific overexpression of PKM2 (pyruvate kinase M2) ameliorated pressure overload-induced heart failure.

A, Schematic illustration of adeno-associated virus type 9-cardiac troponin T-*mPkm2* injection in mice after surgery. **B**, Representative M-mode echocardiography, gross appearance of whole hearts (scale bar, 1 mm), heart cross-sections stained with hematoxylin and eosin (scale bar, 1 mm), histological analysis of heart sections by picrosirius red staining (scale bar, 50 μm) and cell boundaries demarcated with wheat germ agglutinin staining (scale bar, 25 μm) from littermate injected adeno-associated virus type 9-cardiac troponin T-null or adeno-associated virus type 9-cardiac troponin T-*mPkm2* virus 1 week after transverse aortic constriction surgery. **C** and **D**, Quantitative analyses of echocardiography showing ejection fraction, fractional shortening, and heart rate, n=6 to 9. **E**, Statistical results for myocardial interstitial fibrosis analyzed by ImageJ software, n=6 to 9. **F**, Statistical results for the cell cross-sectional area, n=6 to 9. **G**, The ratio of heart weight to body weight, n=6 to 9. **H**, Western blot and quantification of β-MHC, RAC1 (rho family, small GTP binding protein), phosphorylation of p38, p38, phosphorylation of JNK, and JNK expression of cardiomyocyte-specific overexpression of *Pkm2* after transverse aortic constriction surgery. Β-actin served as loading control, n=6. AAV9 indicates adeno-associated virus type 9; β-MHC, β-myosin heavy chain; cTnT, cardiac troponin T; HE, hematoxylin and eosin; HW/BW, heart weight to body weight; *mPkm2* indicates mouse *Pkm2* gene; p-p38, phosphorylation of p38; p-JNK, phosphorylation of JNK; PSR, picrosirius red; TAC, transverse aortic constriction; and WGA, wheat germ agglutinin. Values represent as the mean±SEM, ns, not significant; **P*<0.05, ***P*<0.01, ****P*<0.001, *****P*<0.0001.

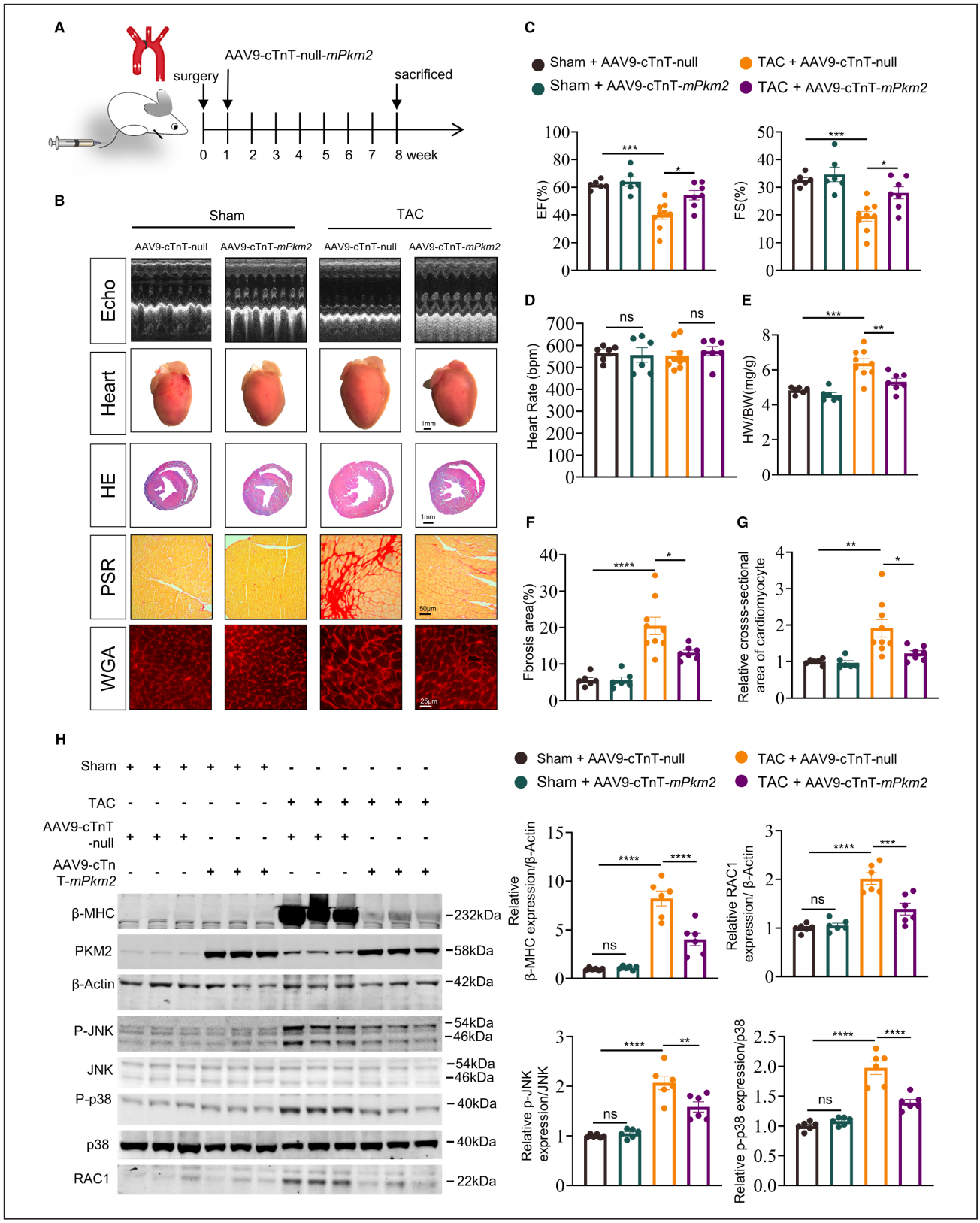

day) or saline for a total of 7 weeks (Figure S5D). One day after the last dose, mice were monitored for echocardiography and the hearts were harvested for subsequent analysis. NSC23766 suppressed TAC-induced RAC1 activation both in *Pkm2*$^{f/f}$-TAC and *Pkm2* cKO-TAC mice (Figure S5E). Moreover, NSC23766 alleviated TAC-induced heart dysfunctions in *Pkm2* cKO mice, including improved cardiac function, lower heart

weight/body weight ratio, smaller cardiomyocytes size, and decreased fibrosis. Though not significant, a trend of improvement in pathological hypertrophy and cardiac function in *Pkm2*$^{f/f}$-TAC mice treated with NSC23766 compared with saline control was observed (Figure 5A through 5E and Figure S5F through S5N). Moreover, NSC23766 drastically reduced β-MHC in both *Pkm2*$^{f/f}$-TAC and *Pkm2* cKO mice (Figure 5F). In total, the significant benefits of NSC23766 on *Pkm2* cKO mice against TAC suggested that the activation of RAC1-MAPK signaling pathway contributed to *Pkm2* deficiency-induced severer cardiac hypertrophy and dysfunction in the pressure-overload heart.

Cardiomyocyte-Specific Overexpression of PKM2 Ameliorated Pressure Overload-Induced HF

To determine the potential protective effect of cardiac PKM2 in the pathological progression under pressure overload, we used a genetic approach using an adeno-associated virus type 9 (AAV9) carrying *Pkm2* gene with a cardiomyocyte-specific cTnT promoter (AAV9-cTnT-*mPkm2*). AAV9-cTnT-null was used as a control. One week after TAC operation, 1 × 10^{11} viral particles/mouse AAV9-cTnT-null or AAV9-cTnT-*mPkm2* virus were injected through the tail vein. Meanwhile, cardiac function was monitored by echocardiography once a week throughout the 8-week experiment period (Figure 6A). At the end point, mice were euthanized, and the heart samples were collected. Both *Pkm2* transcripts (Figure S6A) and protein expression (Figure S6B) were confirmed to be increased significantly after AAV9-cTnT-*mPkm2* injection compared with AAV9-cTnT-null control. The echocardiographic examination showed improved cardiac systolic function without interference on heart rate in mice injected with AAV9-cTnT-*mPkm2* after TAC operation (Figure 6B through 6D and Figure S6C through S6J). Stereomicroscopy, hematoxylin and eosin, wheat germ agglutinin, and picrosirius red staining confirmed that the hearts of TAC mice were significantly enlarged with severer fibrosis compared with sham ones, which was alleviated after AAV9-cTnT-*mPkm2* administration (Figure 6B, 6E and 6F). Meanwhile, there was no significant difference in the ratios of heart weight/body weight between sham- and TAC-operated mice with *Pkm2* overexpression (Figure 6G). In addition, the β-MHC expression was significantly reduced in *Pkm2* overexpression hearts than AAV9-cTnT-null–treated TAC mice (Figure 6H). Contrary to *Pkm2* knockout, *Pkm2* overexpression inhibited hyperactivation of the MAPK signaling pathway in TAC mice hearts (Figure 6H). Taken together, these findings indicated that maintaining a high PKM2 expression may protect the heart against pressure overload-induced hypertrophy and HF.

DISCUSSION

In the present study, we reported that PKM2 exerted cardioprotective effects under pressure overload-induced HF as a protein kinase. Mechanistically, we uncovered that PKM2 inhibited the activation of RAC1-MAPK signaling pathway by phosphorylating RAC1 in cardiomyocytes, which delayed the progression of cardiac hypertrophy and HF. These findings highlighted PKM2 as a prospective target in HF intervention.

Our data demonstrated that *Pkm2* deficiency in cardiomyocytes aggravated hypertrophic growth and cardiac dysfunction both in vitro and in vivo. Conversely, PKM2 overexpression via cardiomyocyte-specific adeno-associated virus (AAV9-cTnT) delivery system effectively delayed HF progression. These results emphasized the crucial role of PKM2 in maintaining heart function homeostasis and validated that the replenishment of PKM2 was a cardioprotective approach for pressure overload-induced HF. As *Pkm2* overexpression was also reported to alleviate myocardial infarction,[15] we conjectured that maintaining a higher level of PKM2 might have universal cardioprotective effects on multifactor-caused heart failure.

Phosphorylation, as a major post-translational protein modification, has been identified in over three quarters of proteins.[39] We observed increased PKM2 protein kinase activity in pressure overload-induced HF, facilitating phosphorylation of RAC1 at S71, which in turn, reduced RAC1 stability. Previous studies have demonstrated that RAC1 activity is critical in cardiomyocyte hypertrophy, cardiomyopathy, heart failure, and arrhythmia.[40] Cardiomyocyte-specific RAC1 deletion or RAC1 inhibitor can prevent myocardial hypertrophy under pressure overload through MAPK pathway inhibition.[38,41] Consistently, our findings revealed that PKM2 deficiency elevated RAC1 expression and exhibited prohypertrophic effects through activation of MAPK pathway (p-p38 and p-JNK). Moreover, upon selective RAC1 inhibitor treatment, TAC-induced cardiac hypertrophy and dysfunction were mitigated in *Pkm2* cKO mice, verifying that RAC1 is one of the main targets of PKM2 in regulating pressure overload-induced HF. Notably, there were other proteins identified as putative PKM2 partners in our immunoprecipitation mass spectrometry data, whose roles in PKM2 deficiency-related cardiomyopathies await further investigation.

PKM2 overexpression was reported to be beneficial in maintaining cardiac function after myocardial infarction.[15] Currently, there have been several strategies for PKM2 maintenance in HF, either by transgenic *Pkm2* overexpression or by small molecules targeting its kinase activity, etc. In particular, small molecules such as Shikonin and TEPP-46 have shown great potentials in treating various diseases including doxorubicin induced cardiotoxicity.[16] Thus, further research targeting

PKM2 to explore new strategies for treatment of pressure overload-induced HF is warranted.

In conclusion, we uncovered a cardioprotective role of PKM2 in maintaining cardiac homeostasis under hemodynamic stress overload. PKM2 protects the heart against pressure overload-induced HF via modulating RAC1-MAPK signaling pathway activity. These new findings will advance our understanding of the pathogenesis of HF and provide a potential therapeutic target for HF.

ARTICLE INFORMATION

Received November 26, 2021; accepted April 28, 2022.

Affiliations

Department of Cardiology, Shanghai East Hospital (L.N., B.L., L.H., M.S., J.Y., D.S.), Key Laboratory of Arrhythmias of the Ministry of Education of China, Shanghai East Hospital (L.N., B.L., L.H., M.S., J.Y., D.S.), and Department of Cell Biology (J.Y.), Tongji University School of Medicine, Shanghai, China; Jinzhou Medical University, Liaoning, China (R.Z., F.F.); and Institute of Medical Genetics, Tongji University, Shanghai, China (J.Y.).

Sources of Funding

This work was funded by the Programs of National Natural Science Foundation of China (82000377 to Dan Shi; 31871491 to Jian Yang).

Disclosures

None.

Supplemental Material

Tables S1–S5
Figures S1–S6

REFERENCES

1. Ziaeian B, Fonarow GC. Epidemiology and aetiology of heart failure. *Nat Rev Cardiol*. 2016;13:368–378. doi: 10.1038/nrcardio.2016.25
2. Maltsev VA, Silverman N, Sabbah HN, Undrovinas AI. Chronic heart failure slows late sodium current in human and canine ventricular myocytes: implications for repolarization variability. *Eur J Heart Fail*. 2007;9:219–227. doi: 10.1016/j.ejheart.2006.08.007
3. Butler J, Yang M, Manzi MA, Hess GP, Patel MJ, Rhodes T, Givertz MM. Clinical course of patients with worsening heart failure with reduced ejection fraction. *J Am Coll Cardiol*. 2019;73:935–944. doi: 10.1016/j.jacc.2018.11.049
4. Nakamura M, Sadoshima J. Mechanisms of physiological and pathological cardiac hypertrophy. *Nat Rev Cardiol*. 2018;15:387–407. doi: 10.1038/s41569-018-0007-y
5. Udelson JE, Stevenson LW. The future of heart failure diagnosis, therapy, and management. *Circulation*. 2016;133:2671–2686. doi: 10.1161/circulationaha.116.023518
6. Zhong W, Cui L, Goh BC, Cai Q, Ho P, Chionh YH, Yuan M, Sahili AE, Fothergill-Gilmore LA, Walkinshaw MD, et al. Allosteric pyruvate kinase-based "logic gate" synergistically senses energy and sugar levels in Mycobacterium tuberculosis. *Nat Commun*. 2017;8:1986. doi: 10.1038/s41467-017-02086-y
7. Zahra K, Dey T, Ashish A, Mishra SP, Pandey U. Pyruvate kinase M2 and cancer: the role of PKM2 in promoting tumorigenesis. *Front Oncol*. 2020;10:159. doi: 10.3389/fonc.2020.00159
8. Verbrugge SAJ, Gehlert S, Stadhouders LEM, Jacko D, Aussieker T, M. J. de Wit G, Vogel ISP, Offringa C, Schönfelder M, Jaspers RT, et al. PKM2 determines myofiber hypertrophy in vitro and increases in response to resistance exercise in human skeletal muscle. *Int J Mol Sci*. 2020;21:7062. doi: 10.3390/ijms21197062
9. Liu T, Kuwana T, Zhang H, Vander Heiden MG, Lerner RA, Newmeyer DD. Phenotypic selection with an intrabody library reveals an anti-apoptotic function of PKM2 requiring Mitofusin-1. *PLoS Biol*. 2019;17:e2004413. doi: 10.1371/journal.pbio.2004413
10. Yuan QI, Miao J, Yang Q, Fang LI, Fang YI, Ding H, Zhou Y, Jiang L, Dai C, Zen KE, et al. Role of pyruvate kinase M2-mediated metabolic reprogramming during podocyte differentiation. *Cell Death Dis*. 2020;11:355. doi: 10.1038/s41419-020-2481-5
11. Chen X, Chen S, Yu D. Protein kinase function of pyruvate kinase M2 and cancer. *Cancer Cell Int*. 2020;20:523. doi: 10.1186/s12935-020-01612-1
12. Yu L, Teoh ST, Ensink E, Ogrodzinski MP, Yang C, Vazquez AI, Lunt SY. Cysteine catabolism and the serine biosynthesis pathway support pyruvate production during pyruvate kinase knockdown in pancreatic cancer cells. *Cancer Metab*. 2019;7:13. doi: 10.1186/s40170-019-0205-z
13. Li C, Zhao Z, Zhou Z, Liu R. PKM2 promotes cell survival and invasion under metabolic stress by enhancing warburg effect in pancreatic ductal adenocarcinoma. *Dig Dis Sci*. 2016;61:767–773. doi: 10.1007/s10620-015-3931-2
14. Wang YU, Zhao H, Guo M, Fei D, Zhang L, Xing M. Targeting the miR-122/PKM2 autophagy axis relieves arsenic stress. *J Hazard Mater*. 2020;383:121217. doi: 10.1016/j.jhazmat.2019.121217
15. Magadum A, Singh N, Kurian AA, Munir I, Mehmood T, Brown K, Sharkar MTK, Chepurko E, Sassi Y, Oh JG, et al. Pkm2 regulates cardiomyocyte cell cycle and promotes cardiac regeneration. *Circulation*. 2020;141:1249–1265. doi: 10.1161/circulationaha.119.043067
16. Saleme B, Gurtu V, Zhang Y, Kinnaird A, Boukouris AE, Gopal K, Ussher JR, Sutendra G. Tissue-specific regulation of p53 by PKM2 is redox dependent and provides a therapeutic target for anthracycline-induced cardiotoxicity. *Sci Transl Med*. 2019;11. doi: 10.1126/scitranslmed.aau8866
17. Zhou L, Miao K, Yin B, Li H, Fan J, Zhu Y, Ba H, Zhang Z, Chen F, Wang J, et al. Cardioprotective role of myeloid-derived suppressor cells in heart failure. *Circulation*. 2018;138:181–197. doi: 10.1161/circulationaha.117.030811
18. Piras BA, Tian Y, Xu Y, Thomas NA, O'Connor DM, French BA. Systemic injection of AAV9 carrying a periostin promoter targets gene expression to a myofibroblast-like lineage in mouse hearts after reperfused myocardial infarction. *Gene Ther*. 2016;23:469–478. doi: 10.1038/gt.2016.20
19. Chen Y, Li X, Li B, Wang HE, Li MS, Huang S, Sun Y, Chen G, Si X, Huang C, et al. Long non-coding RNA ECRAR triggers post-natal myocardial regeneration by activating ERK1/2 signaling. *Mol Ther*. 2019;27:29–45. doi: 10.1016/j.ymthe.2018.10.021
20. Ackers-Johnson M, Li PY, Holmes AP, O'Brien S-M, Pavlovic D, Foo RS. A simplified, Langendorff-free method for concomitant isolation of viable cardiac myocytes and nonmyocytes from the adult mouse heart. *Circ Res*. 2016;119:909–920. doi: 10.1161/circresaha.116.309202
21. Meng D, Lv D-D, Fang J. Insulin-like growth factor-I induces reactive oxygen species production and cell migration through Nox4 and Rac1 in vascular smooth muscle cells. *Cardiovasc Res*. 2008;80:299–308. doi: 10.1093/cvr/cvn173
22. Li R, Sun NA, Chen X, Li X, Zhao J, Cheng W, Hua H, Fukatsu M, Mori H, Takahashi H, et al. JAK2(V617F) mutation promoted IL-6 production and glycolysis via mediating PKM1 stabilization in macrophages. *Front Immunol*. 2020;11:589048. doi: 10.3389/fimmu.2020.589048
23. Ruiz-Villalba A, Mattiotti A, Gunst QD, Cano-Ballesteros S, van den Hoff MJB, Ruijter JM. Reference genes for gene expression studies in the mouse heart. *Sci Rep*. 2017;7:24. doi: 10.1038/s41598-017-00043-9
24. J J. Casson R, P. M. Wood J, Han G, Kittipassorn T, J. Peet D, Chidlow G. M-Type pyruvate kinase isoforms and lactate dehydrogenase a in the mammalian retina: metabolic implications. *Invest Ophthalmol Vis Sci*. 2016;57:66–80. doi: 10.1167/iovs.15-17962
25. Quan C, Li M, Du Q, Chen Q, Wang H, Campbell D, Fang L, Xue B, MacKintosh C, Gao X, et al. SPEG controls calcium reuptake into the sarcoplasmic reticulum through regulating SERCA2a by its second kinase-domain. *Circ Res*. 2019;124:712–726. doi: 10.1161/circresaha.118.313916
26. Huo J-L, Jiao L, An QI, Chen X, Qi Y, Wei B, Zheng Y, Shi X, Gao E, Liu H-M, et al. Myofibroblast deficiency of LSD1 alleviates TAC-induced heart failure. *Circ Res*. 2021;129:400–413. doi: 10.1161/circresaha.120.318149
27. Xia LI, Wang X-R, Wang X-L, Liu S-H, Ding X-W, Chen G-Q, Lu Y. A Novel role for pyruvate kinase M2 as a corepressor for P53 during the DNA damage response in human tumor cells. *J Biol Chem*. 2016;291:26138–26150. doi: 10.1074/jbc.M116.737056
28. Li Y, Lv Z, He L, Huang X, Zhang S, Zhao H, Pu W, Li YI, Yu W, Zhang L, et al. Genetic tracing identifies early segregation of the cardiomyocyte and nonmyocyte lineages. *Circ Res*. 2019;125:343–355. doi: 10.1161/circresaha.119.315280

29. Li Q, Li C, Elnwasany A, Sharma G, An YA, Zhang G, Elhelaly WM, Lin J, Gong Y, Chen G, et al. PKM1 exerts critical roles in cardiac remodeling under pressure overload in the heart. *Circulation*. 2021;144:712–727. doi: 10.1161/circulationaha.121.054885
30. Goldberg MS, Sharp PA. Pyruvate kinase M2-specific siRNA induces apoptosis and tumor regression. *J Exp Med*. 2012;209:217–224. doi: 10.1084/jem.20111487
31. Adam O, Laufs U. Rac1-mediated effects of HMG-CoA reductase inhibitors (statins) in cardiovascular disease. *Antioxid Redox Signal*. 2014;20:1238–1250. doi: 10.1089/ars.2013.5526
32. Brown JH, Del Re DP, Sussman MA. The Rac and Rho hall of fame: a decade of hypertrophic signaling hits. *Circ Res*. 2006;98:730–742. doi: 10.1161/01.RES.0000216039.75913.9e
33. Li P-L, Liu H, Chen G-P, Li L, Shi H-J, Nie H-Y, Liu Z, Hu Y-F, Yang J, Zhang P, et al. STEAP3 (Six-Transmembrane Epithelial Antigen of Prostate 3) inhibits pathological cardiac hypertrophy. *Hypertension*. 2020;76:1219–1230. doi: 10.1161/hypertensionaha.120.14752
34. Custodis F, Eberl M, Kilter H, Böhm M, Laufs U. Association of RhoGDIalpha with Rac1 GTPase mediates free radical production during myocardial hypertrophy. *Cardiovasc Res*. 2006;71:342–351. doi: 10.1016/j.cardiores.2006.04.005
35. Zhao J, Mialki RK, Wei J, Coon TA, Zou C, Chen BB, Mallampalli RK, Zhao Y. SCF E3 ligase F-box protein complex SCF(FBXL19) regulates cell migration by mediating Rac1 ubiquitination and degradation. *Faseb J*. 2013;27:2611–2619. doi: 10.1096/fj.12-223099
36. Zhang B, Zhang P, Tan Y, Feng P, Zhang Z, Liang H, Duan W, Jin Z, Wang X, Liu J, et al. C1q-TNF-related protein-3 attenuates pressure overload-induced cardiac hypertrophy by suppressing the p38/CREB pathway and p38-induced ER stress. *Cell Death Dis*. 2019;10:520. doi: 10.1038/s41419-019-1749-0
37. Blanton RM, Takimoto E, Lane AM, Aronovitz M, Piotrowski R, Karas RH, Kass DA, Mendelsohn ME. Protein kinase g iα inhibits pressure overload-induced cardiac remodeling and is required for the cardioprotective effect of sildenafil in vivo. *J Am Heart Assoc*. 2012;1:e003731. doi: 10.1161/jaha.112.003731
38. Ayuzawa N, Nagase M, Ueda K, Nishimoto M, Kawarazaki W, Marumo T, Aiba A, Sakurai T, Shindo T, Fujita T. Rac1-mediated activation of mineralocorticoid receptor in pressure overload-induced cardiac injury. *Hypertension*. 2016;67:99–106. doi: 10.1161/hypertensionaha.115.06054
39. Sharma K, D'Souza R, Tyanova S, Schaab C, Wiśniewski J, Cox J, Mann M. Ultradeep human phosphoproteome reveals a distinct regulatory nature of Tyr and Ser/Thr-based signaling. *Cell Rep*. 2014;8:1583–1594. doi: 10.1016/j.celrep.2014.07.036
40. Nagase M, Fujita T. Role of Rac1-mineralocorticoid-receptor signalling in renal and cardiac disease. *Nat Rev Nephrol*. 2013;9:86–98. doi: 10.1038/nrneph.2012.282
41. Satoh M, Ogita H, Takeshita K, Mukai Y, Kwiatkowski DJ, Liao JK. Requirement of Rac1 in the development of cardiac hypertrophy. *Proc Natl Acad Sci USA*. 2006;103:7432–7437. doi: 10.1073/pnas.0510444103

Supplemental Material

Table S1. The primer sequences for genotyping.

Primer	Primer sequences
mouse-cre-F	TCTATTGCACACAGCAATCCA
mouse-*cre*-R	CCAGCATTGTGAGAACAAGG
mouse-*Pkm2*$^{f/f}$-F	CCTTCAGGAAGACAGCCAAG
mouse-*Pkm2*$^{f/f}$-R	AGTGCTGCCTGGAATCCTCT

Table S2. The siRNA sequences.

Sequence names	Sequences
Rat-si-*Pkm2*-1-F	CCCUGUGCUGUGUAAGGAU
Rat-si-*Pkm2*-1-R	AUCCUUACACAGCACAGGG
Rat-si-*Pkm2*-2-F	CCCAAGGGCUCCUAUCAUU
Rat-si-*Pkm2*-2-R	AAUGAUAGGAGCCCUUGGG
Rat-si-*Pkm2*-3-F	CGGCAGGAGUGCUCACCAA
Rat-si-*Pkm2*-3-R	UUGGUGAGCACUCCUGCCG
NC-F	GGUUGUGCAAGAGGGCUUU
NC-R	AAAGCCCUCUUGCACAACC
Rat-si-*Rac1*-F	CAAACAGACGUGUUCUUAATT
Rat-si-*Rac1*-R	UUAAGAACACGUCUGUUUGCG
Ms-si-*Pkm1*-F	GUGGAGGCCUCUUAUAAGUTT
Ms-si-*Pkm1*-R	ACUUAUAAGAGGCCUCCACTT

Table S3. The primer sequences for qRT-PCR analysis.

Primer	Primer sequences
mouse/rat-*Pkm2*-F	ATTACCAGCGACCCCACAGAA
mouse/rat-*Pkm2*-R	ACGGCATCCTTACACAGCACA
mouse-*Actb*-F	GGCTGTATTCCCCTCCATCG
mouse-*Actb*-R	CCAGTTGGTAACAATGCCATGT
rat-*Nppb*-F	GTCTCAAGACAGCGCCTTCC
rat-*Nppb*-R	AACCTCAGCCCGTCACAGC
rat-*Myh7*-F	GCGGACATTGCCGAGTCCCAG
rat-*Myh7*-R	GCTCCAGGTCTCAGGGCTTCACA
rat-*18S*-F	GTTGAACCCCATTCGTGAT
rat-*18S*-R	GCTTATGACCCGCACTTACT

Table S4. Antibodies used in this study.

Antibody	Application	Source	Cat No
PKM2	WB	Proteintech	60268-1-Ig
PKM2	WB/IF/IP	Cell Signaling Technology	4053
RAC1	WB/IF/IP	Proteintech	66122-1-Ig
PKM1	WB	Proteintech	15821-1-AP
PKM1	WB	Biorbyt	orb395449
Phospho-Rac1(ser71)	WB	Cell Signaling Technology	2461
P38 MAPK	WB	Cell Signaling Technology	8690
JNK	WB	Cell Signaling Technology	9252
ERK	WB	Cell Signaling Technology	4695
Phospho-P38 MAPK	WB	Cell Signaling Technology	4511
Phospho-JNK	WB	Cell Signaling Technology	4668
Phospho-ERK	WB	Cell Signaling Technology	4370
β-Actin	WB	Santa Cruz	sc-47778
cTnT	IF	Abcam	Ab8295
PKM1/2	WB	Cell Signaling Technology	3190

WB, western blot; IF, immunofluorescence; IP, immunoprecipitation.

Table S5. Immunoprecipitation mass spectrometry in this study.

Accession	Gene name	IP PKM2			IP IgG			AAs	MW [kDa]	pI
		Sum PEP Score	Peptides	Unique Peptides	Sum PEP Score	Peptides	Unique Peptides			
P52480	Pkm	105.772	23	23	20.205	7	7	531	57.8	7.47
A0A2R2Y2P8	TPM1kappa	85.263	23	2	-	-	-	284	32.6	4.73
P53395	Dbt	28.828	12	12	1.569	1	1	482	53.2	8.6
A2ASS6	Ttn	33.826	25	24	7.556	3	3	35213	3904.1	6.2
Q8BGZ7	Krt75	25.334	10	2	-	-	-	551	59.7	8.31
P56480	Atp5f1b	74.134	18	18	57.114	13	13	529	56.3	5.34
B2RX08	Sptb	22.292	13	11	5.503	3	3	2329	267.9	5.49
A0A1L1SV25	Actn4	16.751	5	1	-	-	-	932	107	5.36
P17751	Tpi1	22.866	7	7	6.226	4	4	299	32.2	5.74
E9QQ93	Xirp1	40.656	13	13	24.867	9	9	1132	123.6	5.16
P26041	Msn	13.09	7	3	-	-	-	577	67.7	6.6
P62631	Eef1a2	12.645	5	1	-	-	-	463	50.4	9.03
Q9D2G2	Dlst	15.841	5	5	4.841	3	3	454	49	8.95
P17710	Hk1	13.394	7	7	2.557	2	2	974	108.2	6.8
Q5DTI2	Atp2a2	49.29	18	18	39.361	14	14	1061	116.5	5.5
Q6NXH9	Krt73	9.798	5	1	-	-	-	539	58.9	8.09
Q71LX8	Hsp90ab1	28.721	12	5	19.655	9	4	724	83.2	5.03
J3QQ13	Tnnt2	26.921	9	9	18.229	7	7	302	35.9	5.01

E9Q035	Gm20425	19	9	9	10.518	5	5	978	107.7	7.77
P50544	Acadvl	28.119	11	11	19.784	8	8	656	70.8	8.75
P16546	Sptan1	121.471	45	44	113.731	39	1	2472	284.4	5.33
Q6IME9	Krt72	7.615	4	1	-	-	-	520	56.7	7.4
E9PWQ3	Col6a3	7.224	4	4	-	-	-	3284	353.7	6.93
B7ZCI2	Nebl	13.927	5	5	6.859	4	4	1014	115.9	8.51
Q91YT0	Ndufv1	8.514	4	4	1.638	1	1	464	50.8	8.21
P68510	Ywhah	6.808	3	1	-	-	-	246	28.2	4.89
Q497F1	Tnni3	12.898	4	4	6.198	3	3	211	24.2	9.55
Q9DCV7	Krt7	6.371	4	2	-	-	-	457	50.7	5.87
P47757	Capzb	17.764	9	9	11.554	6	2	277	31.3	5.74
Q60597	Ogdh	11.14	7	7	5.046	4	4	1023	116.4	6.83
Q99LC5	Etfa	14.852	7	7	9.042	4	4	333	35	8.38
Q9CZS1	Aldh1b1	9.032	5	5	3.282	3	3	519	57.5	7.02
P07901	Hsp90aa1	20.82	11	5	15.438	7	2	733	84.7	5.01
Q3TK29	Trap1	5.368	2	1	-	-	-	706	80.1	6.68
Q64727	Vcl	19.136	7	7	13.821	4	4	1066	116.6	6
Q9DCT2	Ndufs3	8.359	3	3	3.099	1	1	263	30.1	7.17
A0A1L1SQ51	Tln2	5.135	2	2	-	-	-	2544	271.8	5.57
P06728	Apoa4	5.071	2	2	-	-	-	395	45	5.47
Q3UAD6	Hsp90b1	9.972	5	4	4.996	3	3	802	92.4	4.82
Q60930	Vdac2	18.735	3	3	14.073	4	4	295	31.7	7.49
Q3TQX5	Ddx3x	4.632	2	2	-	-	-	662	73.1	7.18
P02772	Afp	17.657	7	7	13.265	6	6	605	67.3	5.92

P62242	Rps8	6.352	2	2	2.006	1	1	208	24.2	10.32
E9PWE8	Dpysl3	4.342	3	3	-	-	-	683	73.8	6.46
Q3TEU8	Coro1c	10.349	5	5	6.014	3	3	474	53.1	6.79
Q9JKS4	Ldb3	5.653	2	2	1.46	1	1	723	76.4	7.75
Q9Z0X1	Aifm1	4.072	2	2	-	-	-	612	66.7	9.17
Q7TQ48	Srl	14.883	6	6	10.901	5	5	910	99.1	4.46
P05201	Got1	8.263	4	4	4.334	2	2	413	46.2	7.14
H7BX05	Obscn	4.805	1	1	0.914	1	1	8032	874	5.96
Q80U89	mKIAA0034	10.187	6	6	6.424	3	3	1684	192.4	5.6
A0A0R4J1J1	Pnkd	3.667	1	1	-	-	-	142	15.6	10.27
Q6IRU2	Tpm4	3.635	3	1	-	-	-	248	28.5	4.68
Q99PT1	Arhgdia	3.63	1	1	-	-	-	204	23.4	5.2
Q9CY58	Serbp1	4.996	1	1	1.397	1	1	407	44.7	8.54
P10126	Eef1a1	19.251	7	3	15.686	6	6	462	50.1	9.01
Q5CZY9	Rps16	6.678	3	3	3.123	1	1	172	19.3	10.2
Q01853	Vcp	4.541	2	2	1.011	1	1	806	89.3	5.26
Q3UD06	Atp5c1	16.179	6	6	12.709	5	5	298	32.9	9.01
P61205	Arf3	6.265	2	2	2.883	2	1	181	20.6	7.43
Q3TQP7	Acat1	8.069	4	4	4.746	1	1	424	44.8	8.35
P62751	Rpl23a	5.134	2	2	1.877	1	1	156	17.7	10.45
Q3TIC8	Uqcrc1	8.326	5	5	5.28	2	2	480	52.7	6.1
Q3U6C7	Sucla2	13.441	7	7	10.438	6	6	470	50.6	7.69
Q9D172	D10Jhu81e	4.263	3	3	1.276	1	1	266	28.1	8.78
P45591	Cfl2	4.077	2	2	1.1	1	1	166	18.7	7.88

P38647	Hspa9	28.435	9	9	25.488	8	8	679	73.4	6.07
Q01149	Col1a2	2.875	1	1	-	-	-	1372	129.5	9.19
Q20BD0	Hnrnpab	2.801	1	1	-	-	-	332	36.2	6.95
J3QMG3	Vdac3	13.248	4	3	10.449	2	1	284	30.8	8.79
P97315	Csrp1	2.744	1	1	-	-	-	193	20.6	8.57
P08032	Spta1	7.921	3	2	5.219	3	2	2415	279.7	5.03
Q9QXS6	Dbn1	13.093	6	6	10.393	4	4	706	77.2	4.49
Q3TIE8	Dld	4.632	2	2	1.97	2	2	510	54.6	7.55
Q8R4B4	Dscaml1	2.614	2	2	-	-	-	365	40.5	9.32
Q3TET0	Cct7	3.496	2	2	0.895	1	1	544	59.6	7.84
Q6PB66	Lrpprc	4.597	2	2	1.999	1	1	1392	156.5	6.83
B9EHC7	Casq2	10.377	3	3	7.8	3	3	432	50.1	4.26
O55126	Nipsnap2	5.718	3	3	3.149	1	1	281	32.9	9.26
Q61176	Arg1	2.533	1	1	-	-	-	323	34.8	7.01
Q0PD65	Rab2a	2.529	1	1	-	-	-	212	23.5	6.54
Q80YQ1	Thbs1	2.492	1	1	-	-	-	1171	129.6	4.94
Q3TVM2	Aldh2	3.49	2	2	1.021	1	1	519	56.6	7.36
P17563	Selenbp1	2.438	2	2	-	-	-	472	52.5	6.29
Q3TGZ3	Idh3g	3.301	3	3	0.902	1	1	393	42.8	9.01
Q9D0M3	Cyc1	6.915	3	3	4.535	2	2	325	35.3	9.16
Q62425	Ndufa4	9.507	4	4	7.146	3	3	82	9.3	9.52
Q8C845	Efhd2	12.71	5	5	10.375	4	4	240	26.8	5.14
P08551	Nefl	2.335	2	1	-	-	-	543	61.5	4.64
D9J302	Pdlim5	2.333	2	2	-	-	-	614	66.1	8

Q5FWB6	Rplp0	9.163	4	4	6.833	3	3	317	34.2	6.25
Q05793	Hspg2	2.173	1	1	-	-	-	3707	398	6.32
Q9D6J5	Ndufb8	2.168	1	1	-	-	-	186	21.9	6.64
P56391	Cox6b1	2.162	1	1	-	-	-	86	10.1	8.72
Q91WD5	Ndufs2	4.439	3	3	2.286	2	2	463	52.6	6.99
P19123	Tnnc1	12.715	2	2	10.567	3	3	161	18.4	4.18
Q9D6J6	Ndufv2	2.965	1	1	0.827	1	1	248	27.3	7.4
Q8BH95	Echs1	2.086	1	1	-	-	-	290	31.5	8.48
Q64516	Gk	2.05	1	1	-	-	-	559	61.2	5.87
Q3U9P7	Oxct1	3.476	2	2	1.438	1	1	520	56	8.53
Q3UIJ2	Eif2s3x	2.038	1	1	-	-	-	472	51.1	8.4
P63101	Ywhaz	9.353	3	2	7.371	2	1	245	27.8	4.79
P42125	Eci1	14.214	4	4	12.248	4	4	289	32.2	8.98
P04247	Mb	12.617	2	2	10.667	3	3	154	17.1	7.62
Q8R1S0	Coq6	1.943	1	1	-	-	-	476	51.4	7.17
E9PV24	Fga	9.719	4	4	7.838	4	4	789	87.4	6.11
O88492	Plin4	4.071	2	2	2.214	1	1	1403	139.3	8.59
P51660	Hsd17b4	1.849	1	1	-	-	-	735	79.4	8.57
Q2TPA8	Hsdl2	4.587	2	2	2.76	1	1	490	54.2	6.74
Q7TSF1	Dsg1b	5.712	2	2	3.914	1	1	1060	114.4	4.84
Q9CY64	Blvra	1.779	1	1	-	-	-	295	33.5	7.02
P11531	Dmd	1.682	1	1	-	-	-	3678	425.6	5.94
A0A0G2JFH2	Map4	1.681	1	1	-	-	-	1441	152.7	9.28
P97927	Lama4	1.661	1	1	-	-	-	1816	201.7	6.21

Q9Z1R9	Prss1	1.632	1	1	-	-	-	246	26.1	4.94
Q4FZE6	Rps7	1.601	1	1	-	-	-	194	22.1	10.1
Q3UAG2	Pgd	1.502	1	1	-	-	-	483	53.2	7.23
Q3TIY5	Pkp2	3.37	1	1	1.872	1	1	795	88	9.38
Q8K1M6	Dnm1l	1.491	1	1	-	-	-	742	82.6	7.05
Q9WUR2	Eci2	1.475	1	1	-	-	-	391	43.2	8.92
B9EIU1	Eprs	1.462	1	1	-	-	-	1512	169.9	7.59
Q545A2	Slc25a5	14.824	7	5	13.366	7	3	298	32.9	9.73
Q6RI64	Psmb1	1.458	1	1	-	-	-	240	26.4	7.81
P07309	Ttr	1.456	1	1	-	-	-	147	15.8	6.16
Q3TLP8	**Rac1**	**1.454**	**1**	**1**	-	-	-	**211**	**23.4**	**8.69**
Q3V1M8	Hdlbp	1.447	1	1	-	-	-	1268	141.7	6.87
Q11136	pd	1.422	1	1	-	-	-	493	55	5.78
Q921L4	LOC665622	4.433	2	2	3.019	2	2	135	14.9	10.13
P13020	Gsn	19.396	7	7	18.01	7	7	780	85.9	6.18
Q3UW40	Rpl24	1.38	1	1	-	-	-	160	18.2	11.05
P99029	Prdx5	1.375	1	1	-	-	-	210	21.9	8.85
P47963	Rpl13	1.372	1	1	-	-	-	211	24.3	11.55
Q8BH59	Slc25a12	12.944	7	7	11.58	6	6	677	74.5	8.25
A0A0A0MQA3	Serpina1a	1.364	1	1	-	-	-	436	48.8	6.43
A0A0R4J074	Suv39h2	1.333	1	1	-	-	-	477	54.1	9.04
B7ZW89	Luzp1	1.332	1	1	-	-	-	1110	124.1	7.8
P06745	Gpi	12.157	4	4	10.885	3	3	558	62.7	8.13
Q3TRK9	Slc16a1	7.547	2	2	6.28	2	2	493	53.3	7.47

Q3TRW3	Snd1	1.261	1	1	-	-	-	910	102	7.56
P49813	Tmod1	56.117	13	13	54.916	16	15	359	40.4	5.1
Q9DCT8	Crip2	4.943	3	3	3.759	2	2	208	22.7	8.63
P09103	P4hb	3.024	2	2	1.844	1	1	509	57	4.88
Q4VAG4	Rpl22	5.253	2	2	4.081	1	1	128	14.8	9.19
Q3U8F5	Psmd12	1.169	1	1	-	-	-	456	52.8	7.06
D3YTT6	Osbpl3	1.149	1	1	-	-	-	886	100.4	6.93
P59999	Arpc4	2.447	2	2	1.306	1	1	168	19.7	8.43
P05213	Tuba1b	24.549	8	3	23.412	7	2	451	50.1	5.06
Q9DCX2	Atp5h	8.491	3	3	7.366	3	3	161	18.7	5.69
Q7M6Y5	Deup1	1.123	1	1	-	-	-	601	69.6	6.81
F8VQM8	Xntrpc	1.12	1	1	-	-	-	1264	140.6	8.12
Q91V99	fau	2.595	1	1	1.478	1	1	137	14.8	10.05
P62245	Rps15a	1.057	1	1	-	-	-	130	14.8	10.13
P67778	Phb	13.517	6	6	12.46	5	5	272	29.8	5.76
Q64514	Tpp2	1.056	1	1	-	-	-	1262	139.8	6.58
Q9CZK9	Ppia	2.382	1	1	1.337	1	1	167	18.3	7.9
Q99P72	Rtn4	1.034	1	1	-	-	-	1162	126.5	4.54
Q7TNL3	Stk40	1.032	1	1	-	-	-	435	48.9	7.74
Q69Z91	Acss1	1.014	1	1	-	-	-	683	74.7	6.86
Q3TGR2	Fgb	2.002	2	2	0.997	1	1	481	54.7	7.08
A2AHK0	Dgkz	0.999	1	1	-	-	-	1123	125	8.91
Q3TRR0	Map9	0.987	1	1	-	-	-	646	73.5	7.62
D6Q0F5	Dync1i2	0.986	1	1	-	-	-	655	73.3	5.15

Q6P2K2	Acot2	0.976	1	1	-	-	-	453	49.6	7.62
E9PZI6	Katna1	0.954	1	1	-	-	-	493	56.2	7.5
Q99KW3	Triobp	0.952	1	1	-	-	-	2014	223.2	8.06
A7XUZ6	Skint6	0.942	1	1	-	-	-	1240	141.5	7.17
Q9QYB1	Clic4	1.98	1	1	1.043	1	1	253	28.7	5.59
Q811G0	Bbs9	0.937	1	1	-	-	-	885	99	6.13
B9EK96	Gm15319	0.931	1	1	-	-	-	350	39.5	8.73
Q8CC88	Vwa8	0.923	1	1	-	-	-	1905	213.3	6.6
Q64512	Ptpn13	0.912	1	1	-	-	-	2453	270.2	6.37
P50580	Pa2g4	0.912	1	1	-	-	-	394	43.7	6.86
P97443	Smyd1	0.91	1	1	-	-	-	490	56.5	6.92
A0A0R4J0Q5	Lmnb2	2.976	3	1	2.069	2	1	615	69	5.55
P54775	Psmc4	0.903	1	1	-	-	-	418	47.4	5.21
A2AD39	Stil	0.903	1	1	-	-	-	1262	138.7	6.43
B1AWB9	Col5a1	4.016	2	2	3.127	2	2	1838	183.6	4.98
A0A1B0GR11	Taldo1	0.88	1	1	-	-	-	382	42.1	7.02
P11983	Tcp1	3.528	2	2	2.661	2	2	556	60.4	6.16
Q3TCH2	Uchl1	0.858	1	1	-	-	-	225	25.1	5.33
E9PVY8	Macf1	0.853	1	1	-	-	-	7355	831.4	5.41
Q5SW83	Actr2	0.841	1	1	-	-	-	394	44.7	6.74
Q8R558	Sh3bgr	0.826	1	1	-	-	-	234	25.1	4.08
Q3U280	Vps9d1	0.818	1	1	-	-	-	650	71.3	6.87
E9Q8Q6	Ccdc141	0.816	1	1	-	-	-	1531	173.5	5.88
A0A0G2JGS4	Camk2d	2.226	2	2	1.415	1	1	533	60	7.27

Q571M2	Hspa4	0.806	1	1	-	-	-	930	103.2	5.88
Q02788	Col6a2	0.798	1	1	-	-	-	1034	110.3	6.42
Q8BVQ9	Psmc2	0.795	1	1	-	-	-	475	52.8	6.28
F6QFD1	Pde4d	0.792	1	1	-	-	-	754	85.5	5.25
O88322	Nid2	0.791	1	1	-	-	-	1403	153.8	5.38
Q7TPW6	Slc25a20	0.791	1	1	-	-	-	301	32.9	9.11
Q9D180	Cfap57	0.785	1	1	-	-	-	1249	144.8	5.74
O35948	Wrn	0.782	1	1	-	-	-	643	72.8	8.46
H3BK67	Hmbox1	0.78	1	1	-	-	-	405	45.9	6.33
Q3TA14	Cd36	0.777	1	1	-	-	-	472	52.7	8.35
A0A286YCI8	Sorbs1	0.768	1	1	-	-	-	1290	143	8.31
Q8R2P1	Klhl25	0.761	1	1	-	-	-	589	65.8	6.71
Q8BGH2	Samm50	2.243	2	2	1.504	1	1	469	51.8	6.8
Q6ZPF0	Rab1a	8.382	4	4	7.667	3	2	205	22.7	6.21
P27773	Pdia3	4.871	2	2	4.199	3	3	505	56.6	6.21
E9QNP0	Kxd1	8.781	4	4	8.165	4	4	232	26.8	9.83
Q9Z2I8	Suclg2	4.407	1	1	3.881	1	1	433	46.8	7.02
A0A1S6GWJ8	Hnrnpm	2.606	1	1	2.134	1	1	809	86.4	9.11
Q5XK33	Sdhc	2.035	1	1	1.584	1	1	169	18.4	10.14
Q9JHU4	Dync1h1	1.384	1	1	0.992	1	1	4644	531.7	6.42
Q545C7	Csrp3	2.573	1	1	2.21	1	1	194	20.9	8.54
Q9D051	Pdhb	4.954	2	2	4.614	2	2	359	38.9	6.87
Q5SX53	Slc25a11	13.611	6	6	13.306	4	4	314	34.1	9.94
Q9D881	Gm11273	2.979	1	1	2.698	1	1	129	13.8	8.12

A0A1W2P768	Hist2h3c1	3.721	3	3	3.445	2	2	181	20.2	11.39
Q3UER8	Fgg	1.425	1	1	1.18	1	1	443	50.3	5.62
A0JLY1	Ccdc173	1.529	1	1	1.287	1	1	547	65.1	8.97
P62830	Rpl23	1.045	1	1	0.808	1	1	140	14.9	10.51
Q3UHZ5	Lmod2	1.795	1	1	1.58	1	1	550	62	5.68
Q3US43	Anxa1	2.648	1	1	2.45	2	2	355	40.3	9.03
P61089	Ube2n	1.186	1	1	1.035	1	1	152	17.1	6.57
Q8BMF4	Dlat	1.802	1	1	1.674	1	1	642	67.9	8.57
Q3UPA3	Gdi2	1.557	1	1	1.43	1	1	512	57.7	7.94
A8IP69	Ywhag	5.057	3	1	4.947	3	1	247	28.3	4.89
Q01730	Rsu1	1.099	1	1	1.008	1	1	277	31.5	8.88
P14115	Rpl27a	1.267	1	1	1.217	1	1	148	16.6	11.12
Q3TF40	Nono	0.959	1	1	0.918	1	1	528	60.4	9.61
P11087	Col1a1	0.925	1	1	0.885	1	1	1453	137.9	5.85
P61358	Rpl27	3.732	2	2	3.694	2	2	136	15.8	10.56
Q08189	Tgm3	3.786	1	1	3.756	1	1	693	77.3	6.81
A2AE89	Gstm1	1.786	1	1	1.765	1	1	244	28.5	8.19
Q9D8E6	Rpl4	1.685	1	1	1.689	1	1	419	47.1	11
Q80VP2	Spata7	0.805	1	1	0.814	1	1	582	65.6	6.7
P05202	Got2	8.879	4	4	8.921	3	3	430	47.4	9
Q9CQV8	Ywhab	5.961	3	1	6.009	3	1	246	28.1	4.83
Q3TF25	Atp5o	12.9	5	5	12.999	5	5	213	23.4	9.89
Q9CQ62	Decr1	6.299	2	2	6.4	3	3	335	36.2	8.95
Q3UA52	Arpc2	1.814	1	1	1.922	1	1	383	42.5	9.06

Q6IE21	Otud6a	0.89	1	1	1.009	1	1	290	33.7	7.34
P70349	Hint1	2.197	1	1	2.326	1	1	126	13.8	6.87
P60867	Rps20	2.915	1	1	3.054	1	1	119	13.4	9.94
Q9QXS1	Plec	3.454	2	2	3.597	2	2	4691	533.9	5.96
Q921G7	Etfdh	0.824	1	1	0.99	1	1	616	68	7.58
A0A1S6GWH1	Psmc5	4.338	1	1	4.509	1	1	416	46.6	7.88
Q05C68	Mtch2	1.518	1	1	1.69	1	1	315	34.3	8.75
P60335	Pcbp1	5.181	3	3	5.357	3	2	356	37.5	7.09
P05125	Nppa	1.658	1	1	1.838	1	1	152	16.6	6.55
D3Z4Z0	Tada2b	1.036	1	1	1.23	1	1	420	48.5	7.83
P97461	Rps5	2.166	1	1	2.37	1	1	204	22.9	9.72
Q3THQ5	Stip1	0.865	1	1	1.07	1	1	543	62.5	6.65
Q58EW0	Rpl18	2.686	1	1	2.904	1	1	188	21.6	11.78
Q9CYT6	Cap2	1.464	1	1	1.697	1	1	476	52.8	6.43
Q3TC14	Impa2	2.044	1	1	2.317	1	1	363	38.8	7.44
P61164	Actr1a	1.254	1	1	1.557	1	1	376	42.6	6.64
Q78IK2	Usmg5	2.586	1	1	2.896	1	1	58	6.4	9.83
P24369	Ppib	0.851	1	1	1.176	1	1	216	23.7	9.55
P19324	Serpinh1	15.399	7	7	15.733	6	6	417	46.5	8.82
B2RX02	Zfp692	1.28	1	1	1.62	1	1	531	59	6.95
Q9D023	Mpc2	1.624	1	1	1.973	1	1	127	14.3	10.61
P47934	Crat	9.721	4	4	10.094	6	6	626	70.8	8.44
Q9CQ69	Uqcrq	3.371	2	2	3.768	2	2	82	9.8	10.26
P14069	S100a6	1.324	1	1	1.737	1	1	89	10	5.48

P43277	Hist1h1d	5.79	3	3	6.203	3	1	221	22.1	11.03
A0A0N4SVK8	Adprhl1	2.899	2	2	3.353	1	1	1697	184.1	7.66
Q3V2E0	Try5	1.283	1	1	1.784	1	1	255	27.1	6.73
Q4VAE8	Ndufb4	0.832	1	1	1.358	1	1	131	15.3	9.8
P47857	Pfkm	3.761	3	3	4.291	4	4	780	85.2	8
Q6R0H7	Gnas	2.939	1	1	3.47	1	1	1133	121.4	4.81
P56135	Atp5j2	2.564	1	1	3.105	1	1	88	10.3	9.95
Q920M5	Coro6	9.033	3	3	9.587	3	3	471	52.6	5.96
P18572	Bsg	1.535	1	1	2.193	1	1	389	42.4	5.85
Q9WUM5	Suclg1	3.665	2	2	4.329	1	1	346	36.1	9.39
P48036	Anxa5	1.477	1	1	2.196	1	1	319	35.7	4.96
F8WIV2	Serpinb6a	0.82	1	1	1.555	1	1	399	44.7	6.38
E9PYL9	Gm10036	5.014	2	2	5.765	2	2	178	20.3	9.51
Q3UIM5	Cpt1b	5.967	3	3	6.75	3	3	772	88.1	8.38
P27659	Rpl3	1.772	1	1	2.568	2	2	403	46.1	10.21
Q04857	Col6a1	1.554	1	1	2.352	1	1	1025	108.4	5.36
Q8C266	Rab5c	2.596	1	1	3.433	1	1	234	25.3	8.16
Q3TCP5	Ezr	8.87	5	1	9.727	5	5	586	69.4	6.3
Q9DB79	Rps11	1.598	1	1	2.478	2	2	166	19.4	10.14
Q7TPR4	Actn1	21.972	7	1	22.891	8	2	892	103	5.38
Q3TI05	Cct6a	1.686	1	1	2.658	2	2	531	58	7.08
Q3V0Z8	Ddx5	3.264	1	1	4.261	1	1	690	76.7	8.6
P97807	Fh	8.086	3	3	9.101	4	4	507	54.3	9.04
A0A1Y7VKY1	Gm11361	6.226	3	3	7.249	3	3	152	17.7	10.86

Q4FK74	Atp5d	3.947	1	1	4.983	1	1	168	17.6	5.08
P12787	Cox5a	1.108	1	1	2.151	1	1	146	16.1	6.54
P68040	Rack1	5.198	4	4	6.245	4	4	317	35.1	7.69
Q9CZU6	Cs	2.568	2	2	3.615	2	2	464	51.7	8.57
B2MWM9	Calr	3.673	3	3	4.748	2	2	416	48	4.49
Q9CPQ1	Cox6c	1.628	1	1	2.704	2	2	76	8.5	10.14
P48962	Slc25a4	15.332	7	5	16.436	9	5	298	32.9	9.72
Q3TVV6	Hnrnpu	2.742	2	2	3.875	3	3	800	87.9	6.24
P35700	Prdx1	7.997	4	4	9.174	5	5	199	22.2	8.12
K3W4S6	Gyg	1.23	1	1	2.412	1	1	377	41.9	6.02
P02535	Krt10	23.806	10	8	24.997	9	7	570	57.7	5.11
Q5BLJ7	Rps13	0.98	1	1	2.217	2	2	151	17.2	10.54
Q3TGE1	Actr3	1.1	1	1	2.346	1	1	418	47.4	5.88
P97351	Rps3a	2.148	2	2	3.399	2	2	264	29.9	9.73
F6VW30	Ywhaq	7.818	3	1	9.072	3	1	303	34.3	6.38
P56382	Atp5f1e	1.486	1	1	2.794	2	2	52	5.8	10.01
Q11011	Npps	4.403	2	2	5.788	2	2	920	103.3	5.9
Q99LX0	Park7	0.847	1	1	2.238	2	2	189	20	6.77
Q00623	Apoa1	7.838	4	4	9.305	4	4	264	30.6	5.73
Q9QUM9	Psma6	2.655	1	1	4.139	1	1	246	27.4	6.76
Q99JY0	Hadhb	14.338	6	6	15.827	7	7	475	51.4	9.38
Q6A0D0	Prdx6	1.062	1	1	2.579	2	2	227	25.1	6.37
P10639	Txn	2.902	1	1	4.435	1	1	105	11.7	4.92
Q3TWH2	Nnt	10.313	6	6	11.894	6	6	1086	113.8	7.18

O35129	Phb2	10.609	5	5	12.27	5	5	299	33.3	9.83
P70670	Naca	6.747	2	2	8.434	3	3	2187	220.4	9.35
Q5M9N9	Prdx2	5.498	3	3	7.255	3	3	198	21.8	5.41
O70569	rps14	5.929	2	2	7.719	2	2	151	16.3	10.13
A0A0G2JEX1	Nexn	14.71	10	10	16.535	9	3	671	80	5.22
P62852	Rps25	3.351	2	2	5.244	2	2	125	13.7	10.11
Q3U4U6	Cct3	3.194	1	1	5.13	3	3	545	60.6	6.7
Q9CQA3	Sdhb	6.535	4	4	8.504	4	4	282	31.8	8.68
E9QK41	Ablim1	1.306	1	1	3.28	1	1	861	96.8	8.63
Q9D8N0	Eef1g	1.255	1	1	3.252	2	2	437	50	6.74
Q06185	Atp5i	3.039	1	1	5.07	2	2	71	8.2	9.35
A0A068BFR3	Rab11b	2.966	1	1	5.063	2	2	218	24.5	5.94
A0A075DC90	COX2	5.053	2	2	7.194	3	3	227	26	4.73
Q9JK42	Pdk2	0.824	1	1	2.99	2	2	407	46	6.61
P61750	Arf4	1.004	1	1	3.247	2	2	181	20.5	6.01
E9Q0F0	Krt78	6.667	2	2	8.928	3	1	1068	112.2	7.97
A0A1L1STE6	Idh3a	11.802	6	6	14.074	6	6	384	41.5	6.93
Q60598	Cttn	0.954	1	1	3.237	3	3	546	61.2	5.4
Q678L1	Krt77	15.812	5	1	18.127	5	2	224	26	4.92
Q8VHX6	Flnc	26.907	12	9	29.252	12	9	2726	290.9	5.95
A0A1B0GSX0	Ldha	16.776	8	7	19.151	6	6	361	39.7	8.35
A2AB79	Hist3h2a	7.665	2	2	10.074	3	3	130	14.1	11.05
P62827	Ran	5.108	3	3	7.524	3	3	216	24.4	7.49
P14733	Lmnb1	6.697	4	2	9.194	4	3	588	66.7	5.16

Q60692	Psmb6	1.131	1	1	3.665	2	2	238	25.4	5.11
Q6A0F1	Cct8	2.536	2	2	5.215	3	3	555	60.2	5.62
O55234	Psmb5	2.87	1	1	5.614	2	2	264	28.5	7.02
Q3UK56	Rps3	7.185	3	3	10.005	4	4	243	26.7	9.52
G5E902	Slc25a3	6.119	4	4	8.995	5	5	358	39.7	9.29
Q9WUB3	Pygm	13.954	9	6	16.892	10	6	842	97.2	7.11
Q56A15	Cycs	6.396	2	2	9.45	3	3	105	11.6	9.58
D3Z041	Acsl1	8.026	4	4	11.097	5	5	699	78	7.47
Q9DCW4	Etfb	9.096	4	4	12.181	4	4	255	27.6	8.1
Q6ZWN5	Rps9	2.888	2	2	6.057	4	4	194	22.6	10.65
Q07417	Acads	6.754	3	3	9.969	4	4	412	44.9	8.47
Q6P8J7	Ckmt2	4.824	2	2	8.079	3	3	419	47.4	8.4
Q99KI0	Aco2	28.471	11	11	31.755	12	12	780	85.4	7.93
A0A0A0MQA5	Tuba4a	11.625	6	1	14.96	6	1	477	52.9	5.19
Q91VA7	Idh3b	9.658	4	4	13.173	4	4	384	42.2	8.6
P05132	Prkaca	1.914	1	1	5.441	3	3	351	40.5	8.79
Q5NCI4	Pgam2	7.831	3	3	11.424	3	3	253	28.8	8.5
Q9CQY3	Atp5l	1.909	1	1	5.508	2	2	129	14.2	8.63
P23927	Cryab	9.167	3	3	12.787	6	6	175	20.1	7.33
A2AFQ2	Hsd17b10	0.899	1	1	4.54	2	2	271	28.4	8.76
Q54AH9	Hbb-b2	11.496	4	1	15.174	5	1	146	15.7	8.05
Q9CQB4	Uqcrb	2.696	1	1	6.376	2	2	111	13.6	9.11
P63017	Hspa8	31.379	11	10	35.061	12	5	646	70.8	5.52
Q3TF14	Ahcy	0.797	1	1	4.638	1	1	432	47.7	6.54

Q5M9P3	Rps19	3.744	2	2	7.606	4	4	212	23.1	10.46
O70435	Psma3	1.644	1	1	5.56	2	2	255	28.4	5.44
Q8K3Q4	Actn2	57.109	21	15	61.05	22	16	894	103.9	5.49
P19001	Krt19	11.824	7	2	15.842	8	2	403	44.5	5.39
A0A1S6GWI0	Ndufa8	1.192	1	1	5.292	3	3	206	23.8	9.14
Q546G4	Alb	36.23	15	15	40.353	15	15	608	68.6	6.07
E9Q616	Ahnak	1.952	1	1	6.102	3	3	2106	224	6.46
F6XI62	Rpl7	4.545	3	3	8.736	4	4	279	32.5	11.12
P97350	Pkp1	5.339	3	3	9.532	2	2	728	80.8	8.91
Q76MZ3	Ppp2r1a	2.733	3	3	7.021	3	3	589	65.3	5.11
P62259	Ywhae	7.453	5	4	11.931	4	3	255	29.2	4.74
P31001	Des	41.082	14	11	45.603	14	10	469	53.5	5.27
A0A0R4J083	Acadl	10.167	5	5	14.88	4	4	430	47.9	8.15
P58252	Eef2	6.1	3	3	10.82	5	5	858	95.3	6.83
P21981	Tgm2	3.076	2	2	7.816	4	4	686	77	5.1
P14824	Anxa6	2.595	2	2	7.339	5	5	673	75.8	5.5
Q8BTM8	Flna	15.329	7	5	20.144	8	5	2647	281	6.04
Q3TL71	Hnrnpk	2.622	2	2	7.47	3	3	464	51	5.45
P35492	Hal	0.909	1	1	5.794	3	3	657	72.2	6.34
Q3TFA9	Tmod3	12.208	6	6	17.105	6	5	352	39.4	5.19
P62702	Rps4x	8.017	5	5	12.961	7	7	263	29.6	10.15
P11404	Fabp3	4.966	3	3	9.939	5	5	133	14.8	6.57
P20029	Hspa5	20.342	7	6	25.333	6	5	655	72.4	5.16
A8DUV3	Hbat1	28.977	6	6	34.095	5	5	142	15.1	8.22

Q8C338	Idh1	2.22	1	1	7.434	3	2	422	47.5	6.93
Q3TUI9	Psma5	1.018	1	1	6.323	2	2	241	26.4	4.86
A0A0F7QZE4	HC	24.256	7	6	29.62	6	5	460	50.7	7.77
P19783	Cox4i1	4.932	2	2	10.312	5	5	169	19.5	9.23
Q3UIQ2	Ndufs1	20.991	10	10	26.521	11	11	727	79.7	5.72
P16125	Ldhb	15.36	6	5	20.907	7	7	334	36.5	6.05
A0A2R8VHP3	Gm5478	12.967	7	2	18.614	8	1	535	57.9	6.2
Q9CQR4	Acot13	1.007	1	1	6.723	2	2	140	15.2	8.82
Q9CR68	Uqcrfs1	1.564	1	1	7.373	4	4	274	29.3	8.7
Q3UFJ3	Pdha1	7.771	3	3	13.62	7	7	390	43.2	8.19
Q5FW97	EG433182	13.218	7	7	19.205	8	7	434	47.1	6.8
P14152	Mdh1	4.954	2	2	10.945	4	4	334	36.5	6.58
P09411	Pgk1	10.148	5	5	16.179	6	6	417	44.5	7.9
Q1MWP8	Ehd4	1.98	2	2	8.066	3	3	544	61.6	6.76
O88569	Hnrnpa2b1	8.903	5	5	15.163	6	5	353	37.4	8.95
P48678	Lmna	14.206	8	7	20.478	9	9	665	74.2	6.98
B2CY77	Rpsa	3.009	1	1	9.287	2	2	295	32.8	4.87
P62806	Hist1h4a	7.538	4	4	13.849	5	5	103	11.4	11.36
Q3TFG3	Eif4a1	8.759	4	4	15.164	3	3	406	46.2	5.48
Q9WUZ5	Tnni1	2.499	2	2	9.023	4	4	187	21.7	9.58
Q3TJD4	Atp5f1	4.704	3	3	11.233	5	5	256	28.9	9.26
P54071	Idh2	51.392	15	15	58.022	19	18	452	50.9	8.69
Q0VBK2	Krt80	2.284	2	2	8.93	4	4	452	50.6	6.27
Q3TFQ8	Pygb	13.973	5	2	20.748	9	5	843	96.6	6.65

Q9CQZ5	Ndufa6	1.747	1	1	8.541	2	2	131	15.3	10.11
Q3TXF9	Atp1a1	9.796	5	5	16.647	5	5	1023	112.9	5.39
Q99LC3	Ndufa10	6.507	3	3	13.728	6	6	355	40.6	7.78
Q9DB77	Uqcrc2	36.559	9	9	43.816	11	11	453	48.2	9.25
P45952	Acadm	19.091	7	7	26.485	9	9	421	46.5	8.37
P21550	Eno3	5.89	3	3	13.532	5	4	434	47	7.18
Q9EQD6	K16	24.006	7	3	31.794	9	4	474	52	5.2
Q8BMS1	Hadha	18.348	9	9	26.137	8	8	763	82.6	9.14
Q8BFR5	Tufm	6.635	3	3	14.602	5	5	452	49.5	7.56
P08249	Mdh2	6.915	5	5	14.946	6	6	338	35.6	8.68
Q60932	Vdac1	15.744	5	4	24.321	8	7	296	32.3	8.43
A6ZI44	Aldoa	18.457	10	10	27.163	12	12	418	45.1	7.91
P14602	Hspb1	7.535	3	1	16.618	7	4	82	9.4	5.39
Q9R0Y5	Ak1	1.74	1	1	10.982	3	3	194	21.5	5.81
P63038	Hspd1	23.276	10	10	33.143	12	12	573	60.9	6.18
Q8K2B3	Sdha	9.216	4	4	19.353	8	8	664	72.5	7.37
P04104	Krt1	15.995	7	3	26.839	9	6	637	65.6	8.15
Q542G9	Anxa2	14.454	5	5	26.213	8	8	339	38.7	7.69
P99024	Tubb5	16.671	6	6	28.588	9	2	444	49.6	4.89
E9Q800	Immt	20.221	9	9	32.697	10	10	679	75.6	7.8
Q3UKH3	Acaa2	31.52	11	11	44.587	14	14	397	41.8	8.25
P20152	Vim	45.158	16	13	58.916	18	13	466	53.7	5.12
Q3UIJ3	Actc1	110.913	20	1	125.471	21	3	377	42.1	5.49
P07310	Ckm	6.057	4	4	20.73	7	7	381	43	7.06

Q03265	Atp5f1a	42.488	13	13	57.264	14	14	553	59.7	9.19
P11276	Fn1	10.18	6	6	25.042	11	11	2477	272.4	5.59
Q5DQJ3	Capza2	6.61	3	2	22.134	7	5	286	33	5.85
A8DUL0	Hbbt1	26.13	6	2	42.18	10	5	147	15.8	7.65
Q9QWL7	Krt17	33.087	14	6	49.719	16	2	433	48.1	5.06
B2RTP7	Krt2	20.974	10	6	38.493	15	7	707	70.9	8.06
P50446	Krt6a	34.776	14	5	54.27	20	4	553	59.3	7.94
A0A0A0MQF6	Gapdh	32.879	10	10	52.566	13	13	359	38.6	8.97
Q02257	Jup	15.195	7	7	38.409	15	15	745	81.7	6.14
Q6IFX2	Krt42	28.423	11	6	52.581	17	7	452	50.1	5.16
Q3UV17	Krt76	6.763	4	1	31.095	13	4	594	62.8	8.43
Q3UAS2	Capza1	5.027	3	2	30.441	8	6	290	33.3	6.74
Q32P04	Krt5	44.515	19	10	72.921	28	14	580	61.7	7.75
P21107	Tpm3	44.058	10	1	74.03	20	1	248	28.7	4.72
Q9Z2T6	Krt85	4.448	3	3	35.407	17	4	507	55.7	6.42
Q61765	Krt31	2.335	2	1	33.544	11	4	416	47.1	4.89
P58771	Tpm1	102.836	29	0	135.353	34	3	326	37.4	4.72
Q6PJ18	Tpm2	33.589	13	1	69.019	19	1	284	32.8	4.68
E9Q557	Dsp	45.352	28	28	88.969	43	43	2883	332.7	6.8
Q62261	Sptbn1	19.103	11	1	83.633	28	28	556	64.7	5.27
Q3U804	Actb	3.829	3	1	95.604	18	6	136	15.2	4.65

PEP, Posterior error probability; AAS, number of amino acids in the protein; MW, molecular weight; pI, isoelectric point.

Figure S1. Efficient knockdown of PKM2 in cardiomyocytes and mice hearts.

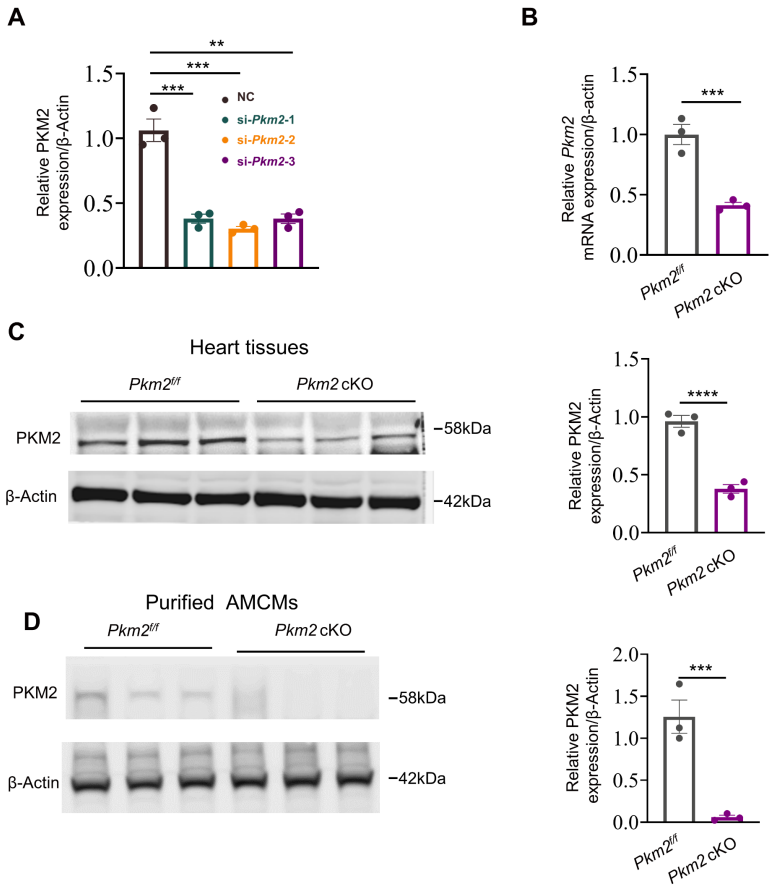

(A) Quantification of the efficiency of interference of three *Pkm2* siRNA sequences assessed by western blot. (B, C) The knockout efficiency of *Pkm2* cKO mice heart tissues assessed by quantitative real-time polymerase chain reaction (qRT-PCR) and western blot. β-Actin served as loading control and each group had at least three biological replicates. (D) Western blot and quantitation of PKM2 in purified adult mouse cardiomyocytes (AMCMs) of *Pkm2*$^{f/f}$ and *Pkm2* cKO mice. β-Actin served as loading control and each group had at least three biological replicates. Values represent as the mean ± SEM, ns, not significant, *P < 0.05, **P < 0.01, ***P < 0.001, ****P < 0.0001.

Figure S2. *Pkm2* cKO mice did not manifest overt developmental and morphological defects in heart.

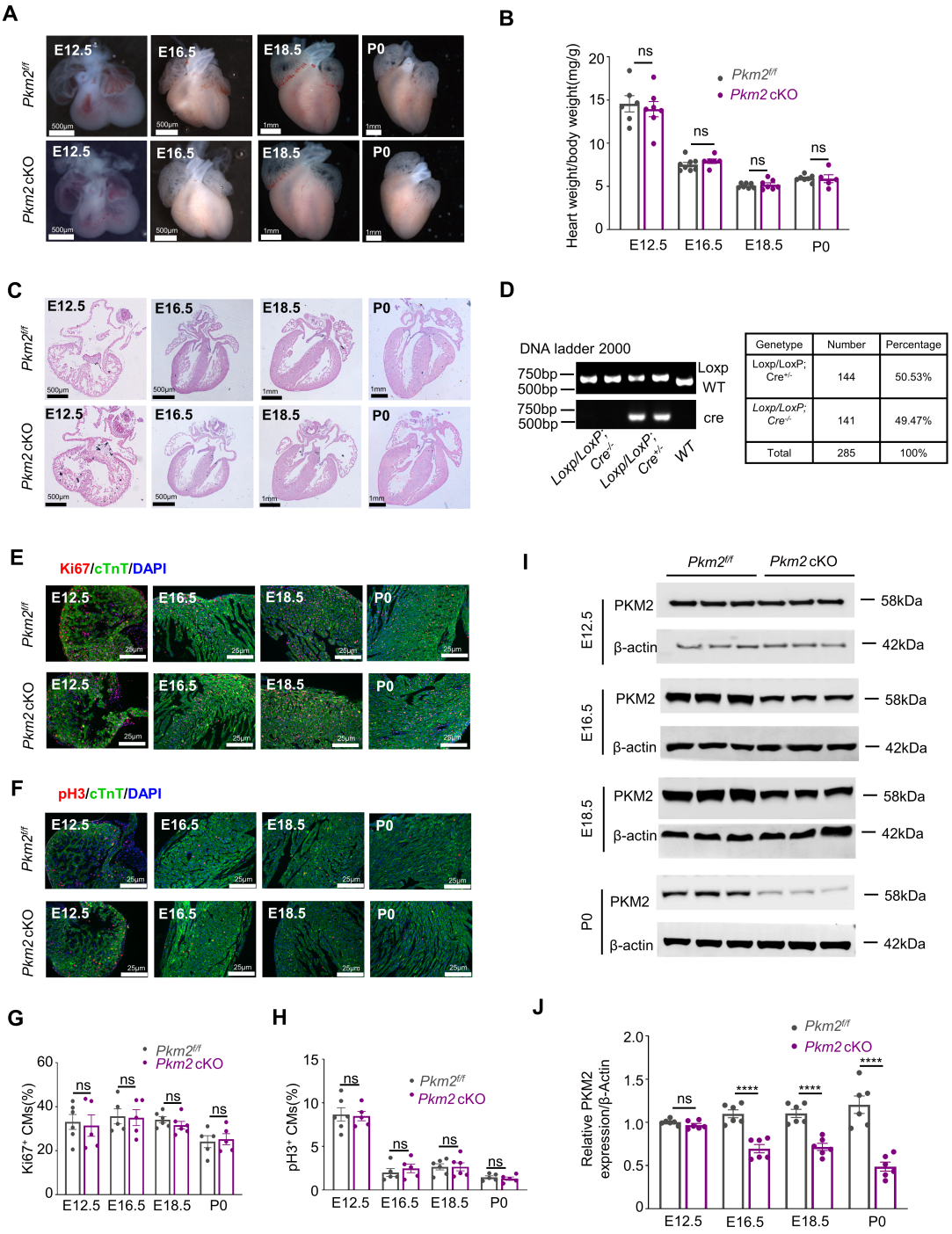

(A-C) Representative gross heart morphology, HE staining and quantification of heart weight to body weight ratio, n = 6 to 8. (D) Viable mice were born at approximately Mendelian ratios. (E, F) Representative images of immunolabeling for Ki67 (red) and pH3 (red) in cardiomyocytes (green). (G, H) The percentages of $Ki67^+$ or $pH3^+$ cardiomyocytes were determined from three sections per

heart, with at least five hearts per group. (I, J) The knockout efficiency of *Pkm2* cKO mice heart tissues assessed by western blot at developmental ages E12.5, E16.5, E18.5 and P0. β-Actin served as loading control, n = 6. Values represent as the mean ± SEM, ns, not significant, *P < 0.05, **P < 0.01, ***P < 0.001, ****P < 0.0001.

Figure S3. Cardiomyocyte-specific *Pkm2* knockout exacerbated pressure overload-induced HF.

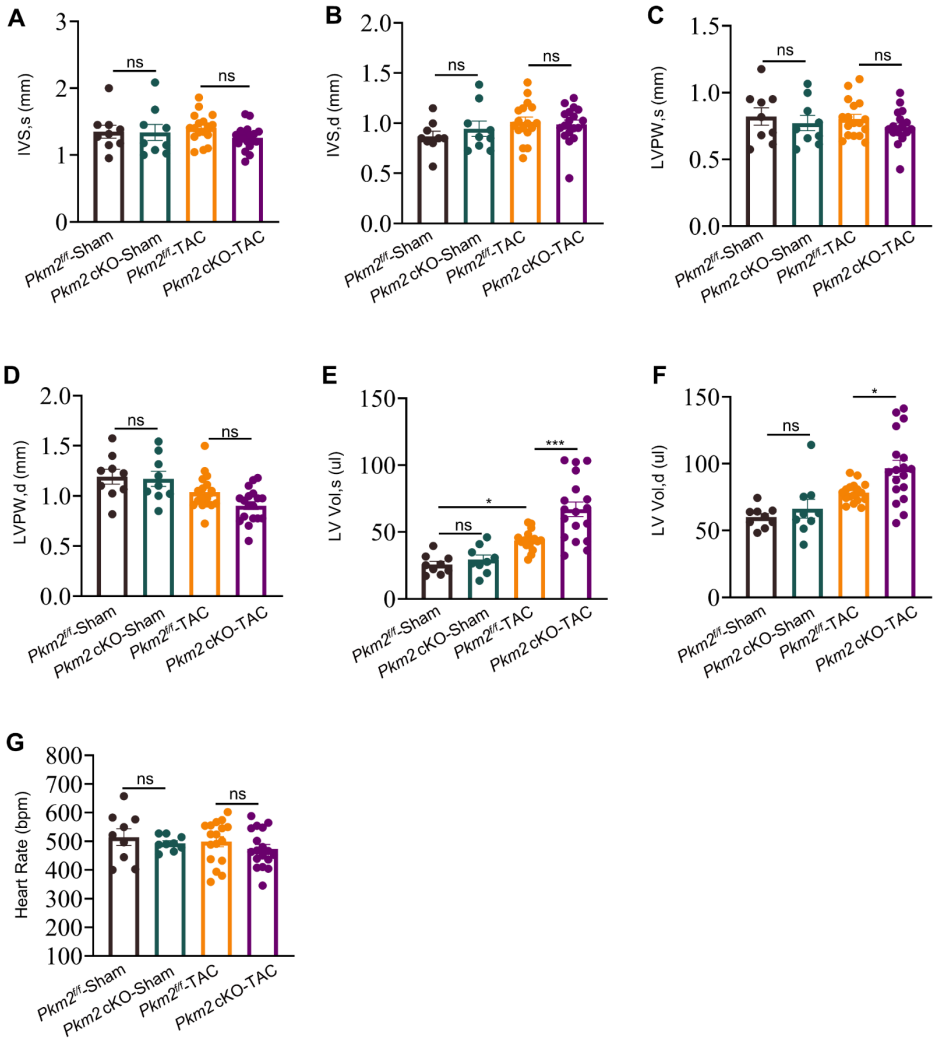

The thickness of systolic (A) and diastolic (B) interventricular septum (IVS,s; IVS,d); the thickness of systolic (C) and diastolic (D) left ventricular posterior wall (LVPW,s; LVPW,d); the systolic (E) and diastolic (F) left ventricular volume (LV vol,s; LV vol,d) and the heart rate (G) of *Pkm2*$^{f/f}$ and *Pkm2* cKO mice after sham or transverse aortic constriction (TAC) surgery by echocardiography, n = 9 to 18. Values represent as the mean ± SEM, ns, not significant, *P < 0.05, **P < 0.01, ***P < 0.001, ****P < 0.0001.

Figure S4. *Pkm1* knockdown exacerbated the phenotype caused by *Pkm2* deficiency in response to pressure overload or PE treatment.

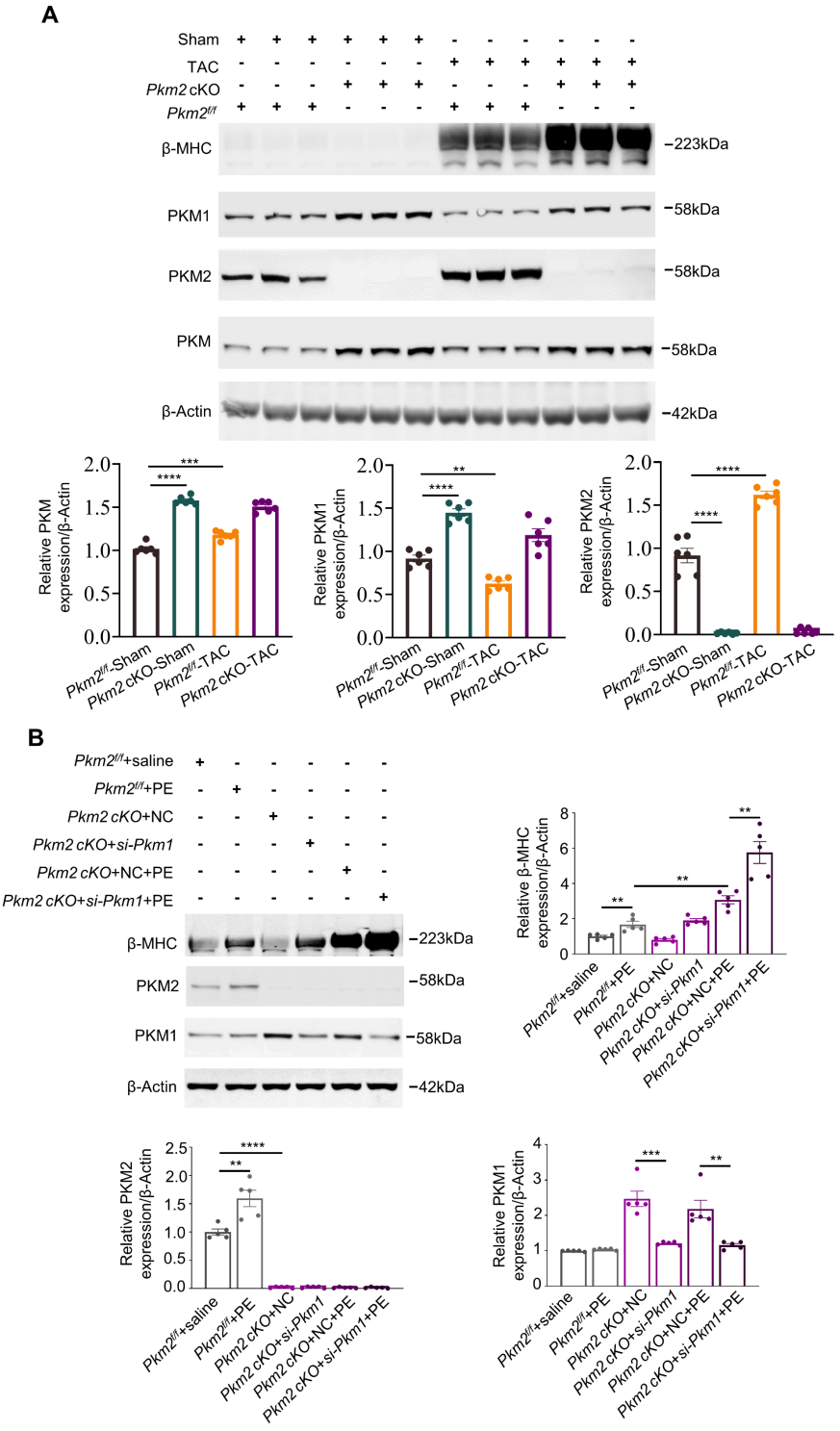

(A) Western blot and quantitation of the expression of PKM, PKM1 and PKM2 in adult mouse cardiomyocytes (AMCMs) purified from *Pkm2*$^{f/f}$ and *Pkm2* cKO mice with or without transverse

aortic constriction (TAC) operation. β-Actin served as loading control, n = 6. (B) Western blot and quantitation of the expression of β-MHC, PKM1 and PKM2 in *Pkm2* cKO AMCMs by siRNA targeting *Pkm1* under phenylephrine (PE) treatment. β-Actin served as loading control, n = 5. Values represent as the mean ± SEM, ns, not significant, *P < 0.05, **P < 0.01, ***P < 0.001, ****P < 0.0001.

Figure S5. Cardiomyocyte-specific *Pkm2* deficiency activated RAC1-MAPK signaling pathway in the progression of HF.

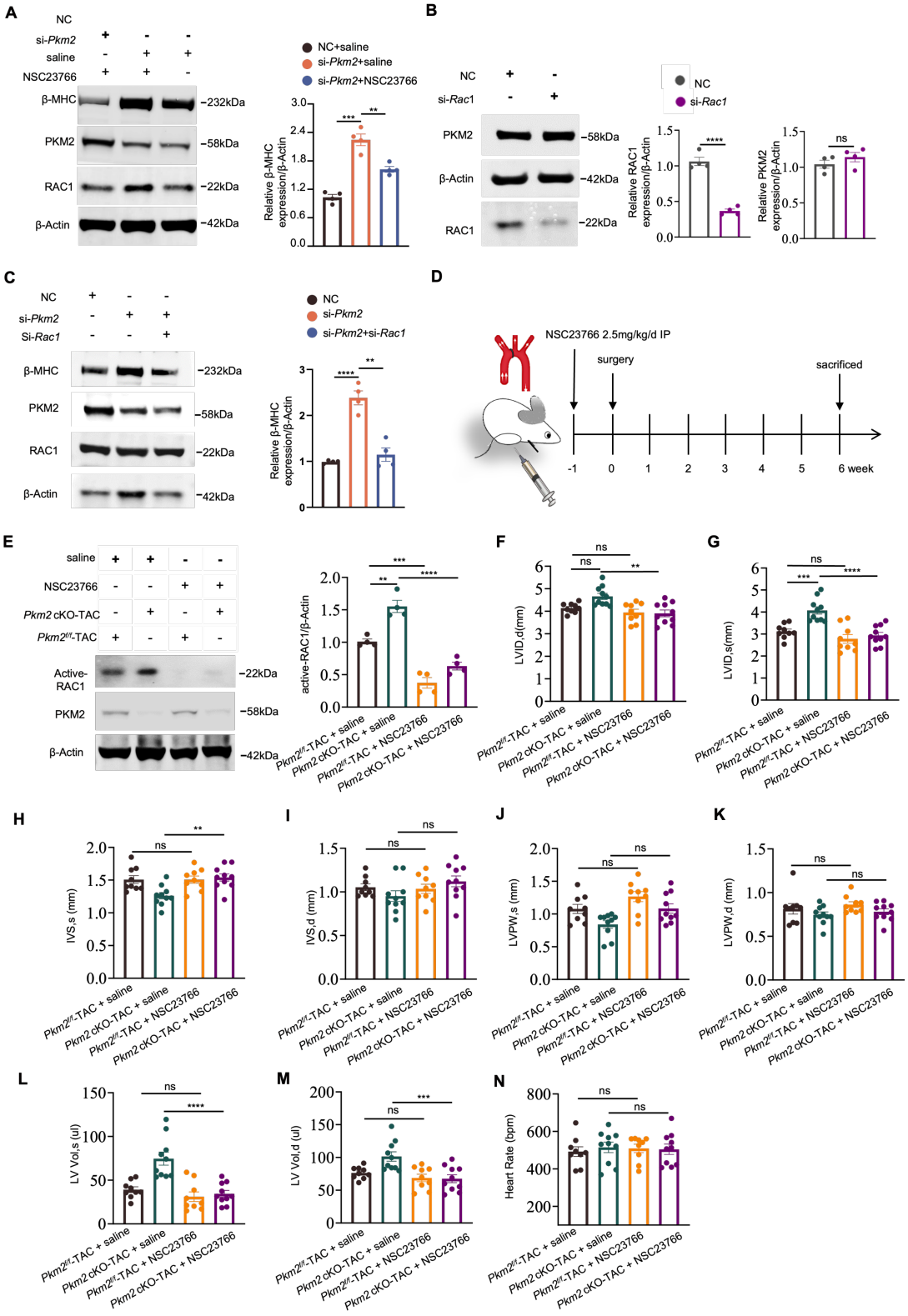

(A) Western blot and quantitation of β-MHC, PKM2 and RAC1 expression after *Pkm2* knockdown

and NSC23766 treatment. β-Actin served as loading control, n = 4. (B) Western blot and quantitation of PKM2 and RAC1 expression after *Rac1* knockdown. β-Actin served as loading control, n = 4. (C) Western blot and quantitation of β-MHC, PKM2 and RAC1 expression after *Pkm2* and *Rac1* knockdown. β-Actin served as loading control, n = 4. (D) Schematic illustration of the NSC23766 administration *in vivo*. (E) Western blot and quantification of active-RAC1 of heart tissue from transverse aortic constriction (TAC)-operated $Pkm2^{f/f}$ and *Pkm2* cKO mice after NSC23766 treatment. β-Actin served as loading control, n = 4. The diastolic (F) and systolic (G) left ventricular internal diameter (LVID,d; LVID,s); the thickness of systolic (H) and diastolic (I) interventricular septum (IVS,s; IVS,d); the thickness of systolic (J) and diastolic (K) left ventricular posterior wall (LVPW,s; LVPW,d); the systolic (L) and diastolic (M) left ventricular volume (LV vol,d; LV vol,s); and heart rate (N) of TAC-operated $Pkm2^{f/f}$ and *Pkm2* cKO mice after NSC23766 treatment by echocardiography, n = 9 to 10. Values represent as the mean ± SEM, ns, not significant, *P < 0.05, **P < 0.01, ***P < 0.001, ****P < 0.0001.

Figure S6. Cardiomyocyte-specific overexpression of PKM2 ameliorated pressure overload-induced HF.

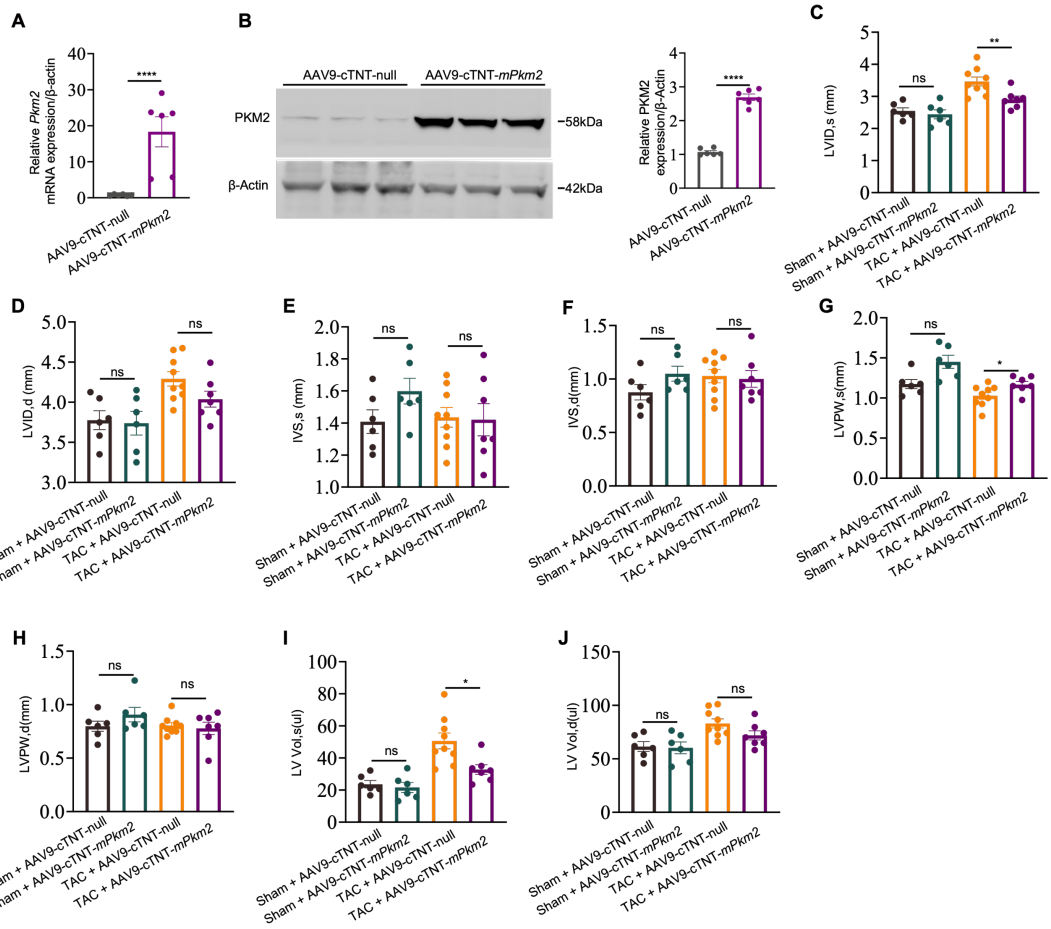

(A, B) The overexpression efficiency of AAV9-cTnT-*mPkm2* virus assessed by quantitative real-time polymerase chain reaction (qRT-PCR) and western blot, n=6. The systolic (C) and diastolic (D) left ventricular internal diameter (LVID,s; LVID,d); the thickness of systolic (E) and diastolic (F) interventricular septum (IVS,s; IVS,d); the thickness of systolic (G) and diastolic (H) left ventricular posterior wall (LVPW,s; LVPW,d); and the diastolic (I) and systolic (J) left ventricular volume (LV vol,s; LV vol,d) of TAC or sham operated mice after *Pkm2* overexpression by echocardiography, n = 6 to 9. Values represent as the mean ± SEM, ns, not significant, *P < 0.05, **P < 0.01, ***P < 0.001, ****P < 0.0001.